



**End-diastolic segmentation of intravascular ultrasound
images enables more reproducible volumetric analysis of
atheroma burden**

Journal:	<i>Catheterization and Cardiovascular Interventions</i>
Manuscript ID	CCI-21-0461.R1
Wiley - Manuscript type:	Original Studies
Keywords:	IVUS - Imaging, Intravascular Ultrasound, ATH - Atherosclerosis, CAD - Coronary Artery Disease

SCHOLARONE™
Manuscripts

1
2
3 **End-diastolic segmentation of intravascular ultrasound images enables more**
4
5 **reproducible volumetric analysis of atheroma burden**
6
7
8
9

10 Emrah Erdogan, MD;^{1,2,3} Xingru Huang, BEng;⁴ Jackie Cooper, MSc;² Ajay Jain, MD;¹ Anantharaman
11 Ramasamy, MBChB;^{1,2} Retesh Bajaj, MBBS, BSc;^{1,2} Ryo Torii, MSc, PhD;⁵ James Moon, MD;^{1,6}
12 Andrew Deaner, MBBS, MD;¹ Christos Costa, MBChB;⁷ Hector M. Garcia-Garcia, MD, PhD;⁸
13 Vincenzo Tufaro, MD;^{1,2} Patrick W. Serruys, MD, PhD;⁹ Francesca Pugliese, MD, PhD;^{1,2} Anthony
14 Mathur, MD, PhD;^{1,2} Jouke Dijkstra, PhD;¹⁰ Andreas Baumbach, MD, PhD;^{1,2} Qianni Zhang PhD;⁴
15 Christos V. Bourantas, MD, PhD^{1,2,6,*}
16
17
18
19
20
21
22
23
24

25 ¹ Department of Cardiology, Barts Heart Centre, Barts Health NHS Trust, London, UK

26
27 ² Centre for Cardiovascular Medicine and Devices, William Harvey Research Institute, Queen Mary
28 University of London, UK
29

30
31 ³ Department of Cardiology, Faculty of Medicine, Yuzuncu Yil University, Van, Turkey
32

33 ⁴ School of Electronic Engineering and Computer Science, Queen Mary University of London, UK
34

35 ⁵ Department of Mechanical Engineering, University College London, London, UK
36

37 ⁶ Institute of Cardiovascular Sciences, University College London, London, UK
38

39 ⁷ Barts and the London School of Medicine and Dentistry, Queen Mary University of London, UK
40

41 ⁸ Department of Cardiology MedStar Washington Hospital Center, Washington, DC, USA
42

43 ⁹ Faculty of Medicine, National Heart & Lung Institute, Imperial College London, UK
44

45 ¹⁰ Department of Radiology, Division of Image Processing, Leiden University Medical Center, Leiden,
46 The Netherlands
47
48
49
50
51

52 **Total Word Count: 5189**
53

54 **Short title:** End-diastolic segmentation for accurate volumetric analysis.
55

56 **Funding:** This study is jointly funded by British Heart Foundation (PG/17/18/32883), University
57 College London Biomedical Resource Centre (BRC492B) and Rosetrees Trust (A1773). EE is funded
58
59
60

1
2
3 by Turkish Society of Cardiology; RB, AR, VT, AM, AB and CVB are funded by Barts NIHR
4 Biomedical Research Centre, London, UK.
5

6
7 **Conflicts of interests:** Professors Anthony Mathur and Andreas Baumbach and Drs Ryo Torii, Qianni
8 Zhang and Christos V. Bourantas hold a patent for the methodology that enables end-diastolic frame
9 detection in intravascular ultrasound (IVUS) images; none of the other authors have a conflict of
10 interest.
11
12
13
14
15
16
17

18 ***Address for correspondence**

19 Dr Christos V. Bourantas MD PhD

20 Consultant Cardiologist, Barts Heart Centre, West Smithfield, London EC1A 7BE

21 E-mail: cbourantas@gmail.com,

22 Phone: +44 203 765 8740
23
24
25
26
27
28
29
30
31
32
33
34
35
36
37
38
39
40
41
42
43
44
45
46
47
48
49
50
51
52
53
54
55
56
57
58
59
60

Abstract

Background: Volumetric intravascular ultrasound (IVUS) analysis is currently performed at a fixed frame interval, neglecting the cyclic changes in vessel dimensions occurring during the cardiac cycle that can affect the reproducibility of the results. Analysis of end-diastolic (ED) IVUS frames has been proposed to overcome this limitation. However, at present, there is lack of data to support its superiority over conventional IVUS.

Objectives: The present study aims to compare the reproducibility of IVUS volumetric analysis performed at a fixed frame interval and at the ED frames, identified retrospectively using a novel deep-learning (DL) methodology.

Methods: IVUS data acquired from 97 vessels were included in the present study; each vessel was segmented at 1mm interval (conventional approach) and at ED frame twice by an expert analyst. Reproducibility was tested for the following metrics; normalised lumen, vessel and total atheroma volume (TAV) and percent atheroma volume (PAV).

Results: The mean length of the analysed segments was 50.0 ± 24.1 mm. ED analysis was more reproducible than the conventional analysis for the normalised lumen (mean difference: 0.76 ± 4.03 mm³ vs 1.72 ± 11.37 mm³; P for the variance of differences ratio < 0.001), vessel (0.30 ± 1.79 mm³ vs -0.47 ± 10.26 mm³; P < 0.001), TAV (-0.46 ± 4.03 mm³ vs -2.19 ± 14.39 mm³; P < 0.001) and PAV ($-0.12 \pm 0.59\%$ vs $-0.34 \pm 1.34\%$; P < 0.001). Results were similar when the analysis focused on the 10mm most diseased segment. The superiority of the ED approach was due to a more reproducible detection of the segment of interest and to the fact that it was not susceptible to the longitudinal motion of the IVUS probe and the cyclic changes in vessel dimensions during the cardiac cycle.

Conclusions: ED IVUS segmentation enables more reproducible volumetric analysis and quantification of TAV and PAV that are established end-points in longitudinal studies assessing the efficacy of novel pharmacotherapies. Therefore, it should be preferred over conventional IVUS analysis as its higher reproducibility is expected to have an impact on the sample size calculation for the primary end-point.

Keywords: Intravascular ultrasound; near-infrared spectroscopy; machine learning.

Introduction

Intravascular ultrasound (IVUS) imaging-based surrogate end-points have been traditionally used to examine the efficacy of novel pharmacotherapies in inhibiting atherosclerotic disease progression (1). Several studies over recent years have used serial IVUS imaging to investigate the role of emerging invasive and non-invasive therapies on vessel wall pathology and plaque evolution. In these reports, IVUS segmentation is traditionally performed at 1mm intervals without taking into account the phase of the cardiac cycle at which these frames are acquired (2-5). However, volumetric analysis with this approach is susceptible to the effect of the longitudinal motion of the IVUS catheter within the vessel and to changes in lumen dimensions during the cardiac cycle which can influence the reported results (6-9). Acknowledging these limitations, in the early days of IVUS, hardware were designed for electrocardiographic (ECG)-gated IVUS image acquisition, and software developed that enabled automated retrospective gating of the IVUS images, taking advantage of the lateral motion of the IVUS catheter in the lumen (10-13). However, these approaches have failed to have broad applications in research as ECG-gated IVUS image acquisition is a time-consuming process, while the developed algorithms for retrospective IVUS gating have not been robustly validated using ECG-estimations as a reference standard, or have not been incorporated in commercially available, user-friendly software. Moreover, there is a lack of data to indicate that IVUS-gated image analysis enables more reproducible quantification of atheroma burden than conventional IVUS segmentation at 1mm interval (14-16). We have recently introduced a novel deep-learning (DL) methodology that is capable of retrospectively detecting the end-diastolic (ED) frames in an IVUS sequence within 15s. The proposed methodology has been incorporated in a user-friendly IVUS-analysis software (QCU-CMS version 4.69; Leiden, University Medical Center, Leiden, The Netherlands), has been validated against ECG-estimations and it has been found to have an excellent accuracy in correctly detecting the ED frames (17). However, the value of this novel DL approach in enabling more reproducible IVUS volumetric analysis has not been explored yet.

Materials and Methods

Study population

1
2
3 We analysed IVUS sequences from patients recruited to the “Evaluation of the efficacy of computed
4 tomographic coronary angiography (CTCA) in assessing coronary artery morphology and physiology”
5 study (NCT03556644). The rationale and study design have been presented previously; in brief, 70
6 patients with stable angina that had obstructive disease on coronary angiography were considered for
7 inclusion. All the patients underwent computed tomography coronary angiography and then were listed
8 for 3-vessel near infrared spectroscopy (NIRS)-IVUS imaging and percutaneous coronary intervention
9 (18). The study protocol complied with the Declaration of Helsinki and was approved by the local
10 research ethics committee; all recruited patients gave written informed consent.
11
12
13
14
15
16
17
18
19
20
21

22 *NIRS-IVUS imaging and segment of interest selection*

23
24 NIRS-IVUS imaging was performed using the Dualpro system (Infraredx, Burlington, Massachusetts,
25 United States). After intracoronary administration of 400mcg nitrates, the NIRS-IVUS catheter was
26 advanced to the distal vessel and an angiographic projection was acquired under contrast dye injection
27 to identify its location within the vessel. Pullback was performed at a constant speed of 0.5mm/s using
28 an automated pullback device at a frame-rate of 30fps. The pullback was completed when the NIRS-
29 IVUS probe entered in the guide catheter. The acquired images were stored in DICOM format and
30 transferred to a workstation for further analysis.
31
32
33
34
35
36
37
38

39 Two interventional cardiologists (CB and AR) reviewed the angiographic images and identified native
40 non-angulated segments that were interrogated by NIRS-IVUS imaging for a length >20mm, exhibited
41 non-flow limiting coronary artery disease – assessed when it was deemed necessary with a fractional
42 flow reserve (FFR) study - and had a lesion/lesions with a maximum diameter stenosis of >20% (15).
43 Segments fulfilling the above criteria were included in the present analysis.
44
45
46
47
48
49
50
51

52 *Conventional versus ED analysis*

53 NIRS-IVUS analysis was performed by an expert analyst whose reproducibility was tested in 20 vessels
54 (supplementary file). Data analysis was performed using two different protocols. In the first, the
55 conventional approach, an expert analyst reviewed the NIRS-IVUS sequence and the angiographic runs
56 and identified the most proximal and distal side-branches that were visible in both NIRS-IVUS and
57
58
59
60

1
2
3 angiographic images to define the segment of interest. NIRS-IVUS segmentation started from a static
4 frame with no motion artifacts portraying the most proximal part of the distal side-branch and was
5 performed at 1mm intervals until the distal end of the proximal side-branch using the QCU-CMS
6 version 4.69 software (Figure 1). In these frames, the lumen and external elastic membrane (EEM)
7 borders were annotated according to the consensus document on the standards for IVUS imaging
8 analysis (15). To examine the reproducibility of this analysis, the identification of the proximal and
9 distal end of the segment of interest and the NIRS-IVUS segmentation was repeated by the same analyst
10 after a 2-month interval.
11
12

13
14 The second approach – the ED analysis – included the inspection of the angiographic and NIRS-IVUS
15 runs and the identification of the proximal and distal end of the segment of interest by the same operator
16 as before. Then, the DL methodology that has been incorporated into the QCU-CMS software and
17 described in the supplementary file was used to identify the ED NIRS-IVUS frames (17). Analysis was
18 performed from the last ED frame portraying the distal side-branch to the first ED frame portraying the
19 proximal side-branch (Figure 1). If the distal side-branch was not visible in the ED frames, then the
20 frame where the side-branch had its largest circumferential extent was identified and analysis started
21 from the first ED frame located after that frame. The same approach was used if the proximal side-
22 branch was not visible in the ED frames; the analysis was ended in the ED frame before the frame where
23 the side-branch had its largest circumferential extent. To evaluate the reproducibility of this analysis,
24 the expert analyst identified the proximal and distal end of the segment of interest and performed the
25 NIRS-IVUS segmentation twice within a 2-month interval.
26
27

28
29 The above validation methodology allows assessment of the reproducibility of the conventional and the
30 ED segmentation in IVUS volumetric analyses, but it is unclear whether variations in the estimated
31 volumes are due to differences in the length of the segment of interest or to the effect of the longitudinal
32 motion of the IVUS catheter and the changes in vessel dimensions occurring during the cardiac cycle.
33 To estimate the effect of the longitudinal motion of the catheter within the vessel and of the changes in
34 lumen dimensions on volume measurements, a fixed-length analysis was performed (supplementary
35 file).
36
37

38
39
40
41
42
43
44
45
46
47
48
49
50
51
52
53
54
55
56
57
58
59
60
Volumetric definitions

1
2
3 The lumen and EEM annotations were used to estimate metrics that have been extensively used in serial
4 intravascular imaging studies of atherosclerosis to examine the effect of novel pharmacotherapies in
5 atherosclerotic disease progression (15). More specially, for each segment of interest, the following
6 metrics were estimated: segment length, lumen volume, EEM volume, total atheroma volume (TAV)
7 and percent atheroma volume (PAV). To account for the differences in the length of the corresponding
8 segments of interest, the normalised lumen, EEM and TAV were estimated as previously described
9 (15). In addition, in each segment of interest, the most diseased 10mm segment – defined as the segment
10 with the largest PAV – was identified, and for this, the lumen, EEM, TAV and PAV were computed.
11
12
13
14
15
16
17
18
19
20
21

22 **Sample size calculation and statistical analysis**

23
24 The study of Jensen et al. is the only report that examined the reproducibility of IVUS segmentation
25 using the conventional 1mm analysis and a prospective ECG-gated pullback approach (14). In this study
26 the mean±standard deviation (SD) of the PAV estimations between the first and second segmentation
27 was $-0.94\pm 3.93\%$ for the conventional and $0.2\pm 3.25\%$ for the ECG-gated analysis. Assuming that in
28 our study the SD for the differences between the first and second segmentation will be 4% for the PAV
29 in the conventional analysis and 3% in the ED analysis, we estimated that we need to include 97
30 segments to prove with a power of 80% and an alpha of 0.05 that ED approach is more reproducible
31 than the conventional approach.
32
33
34
35
36
37
38
39
40

41 Continuous variables are presented as mean±SD, while categorical variables as absolute numbers and
42 percentages. Kolmogorov-Smirnov test was used to examine the distribution of continuous variables; a
43 non-normal distribution was found, and therefore, comparisons between these variables were performed
44 using the Mann Whitney U test, while categorical variables were compared using the chi-square or
45 Fisher's exact test. Bland-Altman analysis, intraclass correlation coefficient (ICC) and variance of
46 difference were used to compare the intra-observer variability in the conventional and ED approach,
47 while the variance ratio was used to compare the reproducibility of the expert between the two
48 approaches. Significance was tested using a robust test for the equality of variances (Brown and
49 Forsythe test). The confidence interval of the variance ratio was estimated using bootstrap re-sampling
50
51
52
53
54
55
56
57
58
59
60

1
2
3 in 1000 samples. Analysis was performed using Stata version 16 (StataCorp, Texas); a P-value <0.05
4
5 was considered statistically significant.
6
7
8

9 **Results**

10 *Studied population*

11
12 Data from 55 out of the 70 patients recruited in the study were included in the present analysis. The
13
14 baseline demographics of the patients and analysed vessels are shown in Table 1. Most of the patients
15
16 were males, had a family history of coronary artery disease, suffered from hypercholesterolemia and
17
18 were in sinus rhythm. The average heart rate was 64 ± 7 (range: 48-78) beats per minute; there was a
19
20 balanced representation of the three coronary arteries in the analysis.
21
22
23
24
25

26 *Conventional versus ED approach*

27
28 The mean length of the analysed segments was 49.96 ± 24.00 mm. In the conventional analyses, the first
29
30 frame of the segment of interest coincided in only 6.19% of the cases, while in the ED analyses in all
31
32 cases. The mean distance difference between the location of the first analysed frame in the two
33
34 conventional analyses was 0.19 ± 0.22 mm, whereas in the ED approach the first frame of the segment of
35
36 interest coincided in all the analyses. The different location of the first frame had an impact on the
37
38 length of the analysed segments; the mean length difference between first and second segmentation in
39
40 the conventional approach was significantly larger than the length difference noted in the ED approach
41
42 (Table 2). The ICC was close to 1 in all the volumetric analyses; however, a larger intra-observer
43
44 variability was noted between the estimations of the expert analyst – as indicated by the variance ratio
45
46 – for the normalised lumen and vessel volumes, TAV and the PAV in the conventional than the ED
47
48 approach (Table 2, Figure 2).
49

50
51 Results were similar for the fixed-length analysis (supplementary file, Table 1, and Figure 3) and when
52
53 the analysis focused on the 10mm most diseased segment. As before, the distance difference between
54
55 the first frame of the most diseased 10mm segment was significantly larger in the conventional than the
56
57 ED analyses (4.96 ± 11.83 mm vs 0.65 ± 4.63 mm, $P<0.001$). The different location of the most diseased
58
59 10mm segment in the two conventional analyses resulted in large differences for the estimated lumen
60

1
2
3 and vessel volumes, TAV and PAV (Table 2). Conversely, in the ED approach, where the location of
4 the 10mm segment coincided in most of the cases, the intra-observer agreement was high for the
5 measured volumes (Table 2).
6
7
8
9

10 11 **Discussion**

12
13 The present study, for the first time, examined the value of a recently introduced DL methodology that
14 allows retrospective identification of ED frames, for improvement of the reproducibility of IVUS
15 volumetric analysis in native coronary arteries. We demonstrated 1) a high intra-observer agreement
16 for normalised lumen and vessel volumes, as well as the TAV and PAV, that have been extensively
17 used as primary end-points in serial IVUS-based studies assessing the efficacy of novel
18 pharmacotherapies on plaque evolution – in the ED approach that is superior to the conventional
19 approach; 2) that these results were consistent when analysis focused on the 10mm most diseased
20 segment which often constitutes a secondary end-point of serial intravascular imaging studies
21 examining the efficacy of emerging therapies in inhibiting plaque evolution, and 3) that the improved
22 reproducibility of the ED analysis is due not only to the fact that it overcomes the errors induced by the
23 longitudinal motion of the IVUS catheter and the changes in the lumen dimensions during the cardiac
24 cycle but also to its superior reproducibility in identifying the segment of interest compared to the
25 conventional approach.
26
27
28
29
30
31
32
33
34
35
36
37
38
39
40

41 Cumulative evidence from the early days of IVUS imaging have demonstrated significant changes in
42 the lumen and vessel dimensions during the cardiac cycle. Ge et al. were the first that systematically
43 examined the changes in the left main stem and left anterior descending artery reporting a pulsatile
44 variation in the lumen cross-sectional area of 10% (8). These results were also confirmed by the study
45 of Weismann et al. who included all the three epicardial coronary arteries and reported an average
46 change in lumen, vessel and plaque area of 8.1%, 3.7% and 4.9% respectively (7). These changes were
47 more prominent in disease-free segments and in segments with non-calcified plaques compared to IVUS
48 frames portraying calcific-rich plaques.
49
50
51
52
53
54
55
56

57 In addition, studies have shown that there is a longitudinal motion of the IVUS probe with regards to
58 the vessel during the cardiac cycle. Arab Zaden et al. have estimated an average longitudinal motion of
59
60

1
2
3 the IVUS probe during the cardiac cycle of 1.50 ± 0.80 mm (range 0.5-5.5mm); while Talou et al.
4 confirmed these findings and showed that the longitudinal motion of the IVUS probe varies depending
5 on the studied vessel (6,9).
6
7

8
9 Therefore, it has been speculated that non-gated IVUS analysis, which neglects the cyclic changes in
10 vessel dimensions and the longitudinal motion of the IVUS catheter within the vessel, has a limited
11 reproducibility in assessing PAV (19). However, this hypothesis was not confirmed by the study of
12 Jensen et al. – the only report that compared the reproducibility of IVUS-gated and non-gated
13 segmentation and reported similar intra-observer agreement. A possible explanation of this paradox is
14 the fact that the study was underpowered in detecting statistically significant differences between the
15 two analyses as it included only 19 coronary artery segments (14). In view of these findings, the current
16 recommendation is to analyse IVUS imaging data neglecting the phase of the cardiac cycle at which
17 these images were acquired (15).
18
19

20
21 The present study examined for the first time the value of ED IVUS segmentation, using a newly
22 developed DL methodology for retrospective ED frame detection, in improving the reproducibility of
23 IVUS analysis. We included an appropriately-powered sample size of 97 vessels that were analysed by
24 an expert analyst twice and demonstrated that the ED analysis improves the intra-observer agreement
25 of the expert for the quantification of the normalised lumen, vessel, TAV and PAV. This was attributed
26 to the higher agreement of the ED analyses for the proximal and distal end of the segment of interest
27 that determine its length but also to the longitudinal displacement of the IVUS probe and the cyclic
28 changes in vessel areas during the cardiac cycle as it was demonstrated in the fixed-length analysis. The
29 value of ED approach was more prominent in the quantification of the TAV and PAV in the 10mm
30 most diseased segment, as the conventional approach had a weak reproducibility in identifying its
31 location in the segment of interest.
32
33

34
35 IVUS imaging has been extensively used over the recent years to assess the effect of novel therapies on
36 PAV and provide mechanistic insights about their implications on plaque morphology (1). In these
37 studies, established pharmacotherapies which appeared effective in improving clinical outcomes had a
38 marginal but consistent effect on PAV, resulting in a PAV reduction that ranged from 0.3-1.4% (2,4,20-
39 22). In this setting, IVUS segmentation is essential to be reproducible as the reliability of a change in
40
41
42
43
44
45
46
47
48
49
50
51
52
53
54
55
56
57
58
59
60

1
2
3 PAV will compound error from both measures, impacting on the required sample size. For example,
4 the observed ICC for the PAV of 0.997 for the ED approach and of 0.985 for the conventional approach
5 would reduce to 0.973 and 0.864 for the change in PAV if we assume that the correlation for the PAV
6 between baseline and follow-up IVUS examinations is 0.89 (23,24); this would result in an 11%
7 reduction in the required sample size by using the more reliable measurement (25). Therefore, in order
8 to detect a 1% reduction in the PAV with an 80% power and 5% alpha, we would need to recruit 111
9 patients if the SD is 1.34% for baseline and follow-up measures and the ICC for PAV is 0.985 – as it
10 was reported in our study with the conventional approach – and 100 patients if the ICC for the PAV
11 improves to 0.997 and the SD to 0.59 with the use of an ED approach. Thus, ED analysis should be
12 considered in serial IVUS-based imaging studies as reducing the sample size is anticipated to decrease
13 their cost and expedite patient recruitment.
14

15
16 The accurate and reproducible quantification of atherosclerotic disease severity using the ED analysis
17 is also likely to enable more accurate estimation of the FFR using IVUS-based computational modelling
18 (26,27). However, this has to be proven in a prospective, appropriately powered clinical study.
19

20 21 22 *Limitations*

23
24 A major limitation of the present study is the fact we tested the reproducibility of the volumetric
25 analyses in IVUS sequences acquired at one time-point and not in sequential IVUS examinations
26 performed during the index procedure as it has been reported in previous analyses (14,28). It is apparent
27 however that the latter would have been possible only in the context of a prospective, large-scale clinical
28 study with pre-specified imaging end-points. Moreover, we did not test the reproducibility of the two
29 approaches to assess changes in the PAV in patients who had IVUS imaging at baseline and after
30 treatment with medications that inhibit atherosclerotic evolution. In addition, the ED analysis is feasible
31 only for IVUS data acquired by a catheter that is withdrawn at low speed as high-speed IVUS pullbacks
32 would result in acquisition of only a handful of end-diastolic IVUS frames per segment. Furthermore,
33 the study was performed using a high-resolution IVUS system so it is unclear whether the reported
34 results would apply to IVUS data acquired by 20MHz or 40MHz IVUS catheters. Moreover, the DL
35 methodology was developed to detect ED frames in patients in sinus rhythm and was tested in this study
36 in a population that was predominantly in sinus rhythm. Further research is needed to examine its
37
38
39
40
41
42
43
44
45
46
47
48
49
50
51
52
53
54
55
56
57
58
59
60

1
2
3 performance in patients with atrial fibrillation and its value in improving the reproducibility of IVUS
4
5 segmentation in this population.
6
7
8

9 **Conclusions**

10 ED IVUS segmentation enables more reproducible IVUS volumetric analysis allowing accurate
11
12 quantification of the normalised lumen, vessel, TAV and the PAV, compared to the conventional
13
14 approach which is currently used by most core-labs. The superiority of ED analysis should be attributed
15
16 to the higher intra-observer agreement in defining the segment of interest but also to the fact that is not
17
18 susceptible to the longitudinal motion of the IVUS catheter and the cyclic changes in vessel dimensions
19
20 during the cardiac cycle. Therefore, the ED approach should be preferred over the conventional
21
22 approach for the analysis of IVUS data acquired in longitudinal studies assessing the efficacy of focal
23
24 and systemic therapies targeting atherosclerosis.
25
26
27
28
29

30 **Data Availability Statement**

31 Data is readily available upon request
32
33
34
35
36
37
38
39
40
41
42
43
44
45
46
47
48
49
50
51
52
53
54
55
56
57
58
59
60

References

1. Bose D, von Birgelen C, Erbel R. Intravascular ultrasound for the evaluation of therapies targeting coronary atherosclerosis. *J Am Coll Cardiol* 2007;49(9):925-32.
2. Nicholls SJ, Ballantyne CM, Barter PJ, Chapman MJ, Erbel RM, Libby P, Raichlen JS, Uno K, Borgman M, Wolski K and others. Effect of two intensive statin regimens on progression of coronary disease. *N Engl J Med* 2011;365(22):2078-87.
3. Nissen SE, Tuzcu EM, Schoenhagen P, Brown BG, Ganz P, Vogel RA, Crowe T, Howard G, Cooper CJ, Brodie B and others. Effect of intensive compared with moderate lipid-lowering therapy on progression of coronary atherosclerosis: a randomized controlled trial. *JAMA* 2004;291(9):1071-80.
4. Nissen SE, Nicholls SJ, Sipahi I, Libby P, Raichlen JS, Ballantyne CM, Davignon J, Erbel R, Fruchart JC, Tardif JC and others. Effect of very high-intensity statin therapy on regression of coronary atherosclerosis: the ASTEROID trial. *JAMA* 2006;295(13):1556-65.
5. Tardif JC, Gregoire J, L'Allier PL, Ibrahim R, Lesperance J, Heinonen TM, Kouz S, Berry C, Bassier R, Lavoie MA and others. Effects of reconstituted high-density lipoprotein infusions on coronary atherosclerosis: a randomized controlled trial. *JAMA* 2007;297(15):1675-82.
6. Arbab-Zadeh A, DeMaria AN, Penny WF, Russo RJ, Kimura BJ, Bhargava V. Axial movement of the intravascular ultrasound probe during the cardiac cycle: implications for three-dimensional reconstruction and measurements of coronary dimensions. *Am Heart J* 1999;138(5 Pt 1):865-72.
7. Weissman NJ, Palacios IF, Weyman AE. Dynamic expansion of the coronary arteries: implications for intravascular ultrasound measurements. *Am Heart J* 1995;130(1):46-51.
8. Ge J, Erbel R, Gerber T, Gorge G, Koch L, Haude M, Meyer J. Intravascular ultrasound imaging of angiographically normal coronary arteries: a prospective study in vivo. *Br Heart J* 1994;71(6):572-8.

- 1
2
3 9. Talou GD, Blanco PJ, Larrabide I, Bezerra CG, Lemos PA, Feijoo RA. Registration Methods
4 for IVUS: Transversal and Longitudinal Transducer Motion Compensation. *IEEE Trans*
5 *Biomed Eng* 2017;64(4):890-903.
6
7
- 8
9 10. von Birgelen C, de Vrey EA, Mintz GS, Nicosia A, Bruining N, Li W, Slager CJ, Roelandt JR,
10 Serruys PW, de Feyter PJ. ECG-gated three-dimensional intravascular ultrasound: feasibility
11 and reproducibility of the automated analysis of coronary lumen and atherosclerotic plaque
12 dimensions in humans. *Circulation* 1997;96(9):2944-52.
13
14
- 15 11. De Winter SA, Hamers R, Degertekin M, Tanabe K, Lemos PA, Serruys PW, Roelandt JR,
16 Bruining N. Retrospective image-based gating of intracoronary ultrasound images for improved
17 quantitative analysis: the intelligate method. *Catheter Cardiovasc Interv* 2004;61(1):84-94.
18
19
- 20 12. Maso Talou GD, Larrabide I, Blanco PJ, Bezerra CG, Lemos PA, Feijoo RA. Improving
21 Cardiac Phase Extraction in IVUS Studies by Integration of Gating Methods. *IEEE Trans*
22 *Biomed Eng* 2015;62(12):2867-77.
23
24
- 25 13. Torbati N, Ayatollahi A, Sadeghipour P. Image-Based Gating of Intravascular Ultrasound
26 Sequences Using the Phase Information of Dual-Tree Complex Wavelet Transform
27 Coefficients. *IEEE Trans Med Imaging* 2019;38(12):2785-2795.
28
29
- 30 14. Jensen LO, Thayssen P. Accuracy of electrocardiographic-gated versus nongated volumetric
31 intravascular ultrasound measurements of coronary arterial narrowing. *Am J Cardiol*
32 2007;99(2):279-83.
33
34
- 35 15. Mintz GS, Garcia-Garcia HM, Nicholls SJ, Weissman NJ, Bruining N, Crowe T, Tardif JC,
36 Serruys PW. Clinical expert consensus document on standards for acquisition, measurement
37 and reporting of intravascular ultrasound regression/progression studies. *EuroIntervention*
38 2011;6(9):1123-30, 9.
39
40
- 41 16. Gerstein HC, Ratner RE, Cannon CP, Serruys PW, Garcia-Garcia HM, van Es GA, Kolatkar
42 NS, Kravitz BG, Miller DM, Huang C and others. Effect of rosiglitazone on progression of
43 coronary atherosclerosis in patients with type 2 diabetes mellitus and coronary artery disease:
44 the assessment on the prevention of progression by rosiglitazone on atherosclerosis in diabetes
45 patients with cardiovascular history trial. *Circulation* 2010;121(10):1176-87.
46
47
48
49
50
51
52
53
54
55
56
57
58
59
60

17. Bajaj R, Huang X, Kilic Y, Jain A, Ramasamy A, Torii R, Moon J, Koh T, Crake T, Parker MK and others. A deep learning methodology for the automated detection of end-diastolic frames in intravascular ultrasound images *Int J Cardiovasc Imaging*. 2021.
18. Ramasamy A, Safi H, Moon JC, Andiapen M, Rathod KS, Maurovich-Horvat P, Bajaj R, Serruys PW, Mathur A, Baumbach A and others. Evaluation of the Efficacy of Computed Tomographic Coronary Angiography in Assessing Coronary Artery Morphology and Physiology: Rationale and Study Design. *Cardiology* 2020;145(5):285-293.
19. De Winter SA, Hamers R, Roelandt JR, Serruys PW, Bruining N. Quantitative gated intravascular ultrasound largely reduces the population size for atherosclerosis progression-regression trials: a computer simulation study. 36th Annual Computers in Cardiology Conference; Park City, UT 2009:829-832.
20. Raber L, Taniwaki M, Zaugg S, Kelbaek H, Roffi M, Holmvang L, Noble S, Pedrazzini G, Moschovitis A, Luscher TF and others. Effect of high-intensity statin therapy on atherosclerosis in non-infarct-related coronary arteries (IBIS-4): a serial intravascular ultrasonography study. *Eur Heart J* 2015;36(8):490-500.
21. Tsujita K, Sugiyama S, Sumida H, Shimomura H, Yamashita T, Yamanaga K, Komura N, Sakamoto K, Oka H, Nakao K and others. Impact of Dual Lipid-Lowering Strategy With Ezetimibe and Atorvastatin on Coronary Plaque Regression in Patients With Percutaneous Coronary Intervention: The Multicenter Randomized Controlled PRECISE-IVUS Trial. *J Am Coll Cardiol* 2015;66(5):495-507.
22. Nicholls SJ, Puri R, Anderson T, Ballantyne CM, Cho L, Kastelein JJ, Koenig W, Somaratne R, Kassahun H, Yang J and others. Effect of Evolocumab on Progression of Coronary Disease in Statin-Treated Patients: The GLAGOV Randomized Clinical Trial. *JAMA* 2016;316(22):2373-2384.
23. Nissen SE, Tuzcu EM, Libby P, Thompson PD, Ghali M, Garza D, Berman L, Shi H, Buebendorf E, Topol EJ and others. Effect of antihypertensive agents on cardiovascular events in patients with coronary disease and normal blood pressure: the CAMELOT study: a randomized controlled trial. *JAMA* 2004;292(18):2217-25.

- 1
2
3 24. May K, Hittner JB. On the relation between power and reliability of difference scores. *Percept*
4 *Mot Skills* 2003;97(3 Pt 1):905-8.
5
6
7 25. Perkins DO, Wyatt RJ, Bartko JJ. Penny-wise and pound-foolish: the impact of measurement
8 error on sample size requirements in clinical trials. *Biol Psychiatry* 2000;47(8):762-6.
9
10
11 26. Yu W, Tanigaki T, Ding D, Wu P, Du H, Ling L, Huang B, Li G, Yang W, Zhang S and others.
12 Accuracy of Intravascular Ultrasound-Based Fractional Flow Reserve in Identifying
13 Hemodynamic Significance of Coronary Stenosis. *Circ Cardiovasc Interv* 2021;14(2):e009840.
14
15
16 27. Sakurai S, Takashima H, Waseda K, Gosho M, Kurita A, Ando H, Maeda K, Suzuki A,
17 Fujimoto M, Amano T. Influence of plaque characteristics on fractional flow reserve for
18 coronary lesions with intermediate to obstructive stenosis: insights from integrated-backscatter
19 intravascular ultrasound analysis. *Int J Cardiovasc Imaging* 2015;31(7):1295-301.
20
21
22
23
24
25
26 28. Rodriguez-Granillo GA, Vaina S, Garcia-Garcia HM, Valgimigli M, Duckers E, van Geuns RJ,
27 Regar E, van der Giessen WJ, Bressers M, Goedhart D and others. Reproducibility of
28 intravascular ultrasound radiofrequency data analysis: implications for the design of
29 longitudinal studies. *Int J Cardiovasc Imaging* 2006;22(5):621-31.
30
31
32
33
34
35
36
37
38
39
40
41
42
43
44
45
46
47
48
49
50
51
52
53
54
55
56
57
58
59
60

Figure legends

Figure 1. A case example showing the segment of interest defined by the conventional and the ED approach. In the ED approach, the proximal and distal end of the segment of interest coincide; conversely, in the conventional approach there was 3 frame difference between the estimations of the expert analyst for the location of the distal end of the segment of interest.

Figure 2. Bland-Altman plots of the % differences of the estimations of the expert analyst for the normalised lumen, vessel, TAV and the PAV in the conventional analysis (A, B, C and D respectively) and ED analysis (E, F, G and H respectively).

Supplementary Figure 1. Methodology applied to identify the 10 sub-segments that will be used to define the distal end of the segment of interest in the second fixed-length analysis using the conventional approach. After the detection of the most distal ED frame – i.e., the frame at the peak of the QRS complex – of the segment of interest using the DL methodology, then the cardiac cycle was split to 10 sub-segments; 5 sub-segments were defined distally and 4 proximally to the ED frame. One of these frames will be considered as the distal end of the segment of interest in the second fixed-length analysis using the conventional approach.

Supplementary Figure 2. Segment of interest defined by the ED and the conventional approach in the fixed-length analysis. The distal end of the segment of interest was similar in the two ED analyses and the 1st conventional analysis. In the 2nd conventional analysis, the distal end of the segment of interest was located 3 frames more proximally – corresponding to the first sub-segment of the period between two end-diastolic frames.

Supplementary Figure 3. Bland-Altman plots of the % differences of the estimations of the expert analyst for the normalised lumen, vessel, TAV and the PAV in the fixed-length analyses for the conventional (A, B, C and D respectively) and the ED approaches (E, F, G and H respectively).

Supplement

End-diastolic segmentation of intravascular ultrasound images enables more reproducible volumetric analysis of atheroma burden

Emrah Erdogan, MD;^{1,2,3} Xingru Huang, BEng;⁴ Jackie Cooper, MSc;² Ajay Jain, MD;¹ Anantharaman Ramasamy, MBChB;^{1,2} Retesh Bajaj, MBBS, BSc;^{1,2} Ryo Torii, MSc, PhD;⁵ James Moon, MD;^{1,6} Andrew Deaner, MBBS, MD;¹ Christos Costa, MBChB;⁷ Hector M. Garcia-Garcia, MD, PhD;⁸ Vincenzo Tufaro, MD;^{1,2} Patrick W. Serruys, MD, PhD;⁹ Francesca Pugliese, MD, PhD;^{1,2} Anthony Mathur, MD, PhD;^{1,2} Jouke Dijkstra, PhD;¹⁰ Andreas Baumbach, MD, PhD;^{1,2} Qianni Zhang PhD;⁴ Christos V. Bourantas, MD, PhD^{1,2,6,*}

¹ Department of Cardiology, Barts Heart Centre, Barts Health NHS Trust, London, UK

² Centre for Cardiovascular Medicine and Devices, William Harvey Research Institute, Queen Mary University of London, UK

³ Department of Cardiology, Faculty of Medicine, Yuzuncu Yil University, Van, Turkey

⁴ School of Electronic Engineering and Computer Science, Queen Mary University of London, UK

⁵ Department of Mechanical Engineering, University College London, London, UK

⁶ Institute of Cardiovascular Sciences, University College London, London, UK

⁷ Barts and the London School of Medicine and Dentistry, Queen Mary University of London, UK

⁸ Department of Cardiology MedStar Washington Hospital Center, Washington, DC, USA

⁹ Faculty of Medicine, National Heart & Lung Institute, Imperial College London, UK

¹⁰ Department of Radiology, Division of Image Processing, Leiden University Medical Center, Leiden, The Netherlands

*Address for correspondence

Dr Christos V. Bourantas MD PhD

Consultant Cardiologist, Barts Heart Centre, West Smithfield, London EC1A 7BE

E-mail: cbourantas@gmail.com, Phone: +44 203 765 8740

Materials and Methods

DL methodology for ED frame detection

The developed DL methodology for retrospective ED frame detection was trained in NIRS-IVUS imaging data that were co-registered with the concurrent electrocardiographic (ECG)-signal and were acquired from 20 coronary artery segments. The ECG estimations for the ED were used as the reference standard.

The methodology is based on a network model with a bidirectional gated-recurrent-unit (Bi-GRU) structure. The model analyses the whole IVUS sequences to determine patterns of changes in pixel intensity in corresponding pixels between consecutive frames to identify the frame corresponding to ED.

First, the IVUS sequence is pre-processed by a median filter to reduce noise and then the absolute pixel-intensity difference between corresponding pixels in consecutive IVUS frames is calculated and added for each frame across the entire pullback; these data which represents the relative motion of the vessel in relation to the IVUS probe are smoothed by a Hanning smoothing algorithm. The processed values are analyzed by the DL model. A 64-frame segment window is generated that is scanned by a Bi-GRU model which analyses patterns of the changes in pixel intensity to identify the ED frame. This window advances frame by frame sequentially until the entire IVUS pullback is analyzed. For each segment window, the probability that the 32nd frame is the ED frame is calculated; the frames with the highest probability amongst neighboring frames are selected and constitute the network output.

Testing of the DL in the same dataset using the leave-one-out approach demonstrated that the proposed method had an excellent accuracy of 80.4% in correctly detecting the ED frame (1).

Intra- and inter-observer variability of the expert analyst

The intra- and inter-observer variability of the expert analyst for the lumen and EEM borders was examined in 2,437 ED frames obtained from 20 vessels. The analyst detected these borders twice within a 2-month interval and the area estimations between the two analyses were compared. The same dataset was segmented by another expert, and his estimations were compared with the estimations of the first analyst to report the inter-observer variability.

1
2
3 An excellent agreement between expert analyst estimations was found for the lumen and EEM areas
4 (mean difference: $0.07 \pm 0.47 \text{mm}^2$ and $0.09 \pm 0.46 \text{mm}^2$ respectively). The inter-observer agreement of the
5 two experts was also high with the mean difference between observers' estimations being $0.07 \pm 0.65 \text{mm}^2$
6 for the lumen and $0.10 \pm 0.53 \text{mm}^2$ for the EEM areas.
7
8
9
10

11 12 13 *Fixed-length analysis using the conventional and the ED approach*

14
15 To estimate the effect of the longitudinal motion of the catheter within the vessel and of the changes in
16 lumen dimensions on volume measurements two analyses were performed.
17

18
19 In the first, the expert analyst identified the ED frame that corresponded to the distal end of the segment
20 of interest and then analysis was performed at 1mm intervals till its proximal end that corresponded to
21 the frame portraying the most distal part of the most proximal side-branch.
22
23
24

25
26 The second analysis started from a phase of the cardiac cycle that was not necessarily the ED phase.
27 More specifically, the distal end of the segment of interest in this analysis was estimated using the
28 following approach: the heart rate in each pullback was used to identify the frame interval between two
29 ED frames and this was split in 10 sub-segments. For example, if the heart rate of a patient was 60 beats
30 per minute and the catheter acquired 30 fps then the frame interval between two ED frames is 30 frames
31 and each one of the 10 sub-segments has 3 frames.
32
33
34
35
36
37

38
39 Then, 5 sub-segments were defined distally and 4 proximally to the ED frame that corresponded to the
40 distal end of the segment of interest in the first analysis so as the beginning of the second analysis to be
41 close to the first. The frames at the end of the above 10 sub-segments (5 before the ED frame, 1 at ED
42 and 4 proximally to the ED) portrayed the vessel at 10 different phases of the cardiac cycle
43 (Supplementary Figure 1).
44
45
46
47
48

49
50 In order to have an equal representation of these 10 phases in the second analysis, we implemented the
51 following process: for the first vessel the distal end of the second analysis corresponded to the frame at
52 the end of the 5th sub-segment located distally to the most distal ED frame of the first analysis, for the
53 second vessel the distal end of the second analysis corresponded to the frame at the end of the 4th sub-
54 segment, for the 3rd vessel to the 3rd sub-segment and so on till the 10th vessel for which the distal end
55 of the analysis corresponded to the frame at the end of the 4th sub-segment located proximally to the
56
57
58
59
60

1
2
3 distal ED frame of the first analysis. This process was repeated sequentially for all the studied vessels.
4
5 The proximal end of the segment of interest in the second analysis was estimated in such a way so as its
6
7 length to be equal to the length of this segment in the first analysis (Supplementary Figure 2).
8
9 The reproducibility of the above-mentioned fixed-length conventional analysis was compared with the
10
11 reproducibility of a fixed-length ED analysis. For this purpose, the expert analyst performed twice the
12
13 segmentation of the ED frames, identified by the developed DL approach, that were included in the
14
15 segment of interest which was assumed to have a fixed length.
16
17
18
19
20

21 **Results**

22 *Fixed-length analysis with the conventional and the ED approach*

23
24 Supplementary Table 1 shows the results of the fixed-length analyses for the conventional and the ED
25
26 approaches. A high ICC was noted for all the measurements in both approaches. However, the mean±SD
27
28 of the differences between the two analyses were smaller in the ED approach for all the studied metrics,
29
30 while the variance ratio indicated that this methodology enables more reproducible volumetric analysis
31
32 than the conventional approach (Supplementary Figure 3).
33
34
35
36
37
38
39
40
41
42
43
44
45
46
47
48
49
50
51
52
53
54
55
56
57
58
59
60

References

1. Bajaj R, Huang X, Kilic Y, Jain A, Ramasamy A, Torii R, Moon J, Koh T, Crake T, Parker MK and others. A deep learning methodology for the automated detection of end-diastolic frames in intravascular ultrasound images Int J Cardiovasc Imaging. 2021

For Review Only

Tables

Table 1. Baseline demographics of the studied patients.

	Studied patients (n=55)
Age (years)	62±8
Gender (male)	41 (75%)
Smoking history	29 (53%)
Family history of CAD	33 (60%)
Previous acute coronary syndrome	7 (13%)
Co-morbidities	
Diabetes mellitus	18 (33%)
Hypertension	29 (53%)
Hypercholesterolemia	37 (67%)
Atrial fibrillation	5 (9%)
Renal failure*	0 (0%)
Anemia	0 (0%)
Previous PCI	12 (22%)
LV function**	
Normal LV function	51(93%)
Impaired LV function	4 (7%)
Studied vessels	
(n=97)	
Left anterior descending artery/diagonal branch	32 (33%)
Left circumflex artery/obtuse marginal branch	33 (34%)
Right coronary artery	32 (33%)

***Table footnote:** CAD, coronary artery disease; LV, left ventricle; PCI, percutaneous coronary intervention.

*Renal failure was defined as an estimated glomerular filtration rate of <60ml/min/1.73m².

** Impaired LV function was defined as LV ejection fraction <50%.

Table 2. Comparison of the estimations of the conventional and the ED analysis for the length of the segment of interest, the normalised lumen, vessel volumes, TAV and PAV.

	1 st 1mm analysis	2 nd 1mm analysis	Δ	ICC*	Variance of difference*	1 st ED analysis	2 nd ED analysis	Δ	ICC*	Variance of difference**	Variance ratio (95% CI)	P**
Segment of interest analysis												
Length (mm)	49.62±23.90	49.57±23.83	0.05±0.36	1.000	0.131	49.96±24.0	49.97±24.05	0.00±0.04	1.000	0.002	65.7 (19.8-111.6)	<0.001
Lumen volume (mm ³)	398.8±264.9	397.08±264.7	1.72±11.37	0.999	129.3	406.2±268.9	405.4±268.7	0.76±4.03	1.000	16.24	7.96 (1.37-14.54)	<0.001
Vessel volume (mm ³)	647.5±426.2	648.00±429.3	-0.47±10.26	1.000	105.3	653.4±429.9	653.1±429.4	0.30±1.79	1.000	3.20	32.9 (22.0-49.1)	<0.001
TAV (mm ³)	248.7±173.6	250.93±176.2	-2.19±14.39	0.997	297.07	247.2±173.4	247.7±173.3	-0.46±4.03	1.000	16.24	5.61 (2.85-8.38)	<0.001
PAV (%)	37.83±7.89	38.17±7.88	-0.34±1.34	0.985	1.79	37.38±7.96	37.49±7.91	-0.12±0.59	0.997	0.35	5.11 (2.34-7.90)	<0.001
Most diseased 10mm segment analysis												
Lumen volume (mm ³)	69.6±30.7	68.6±29.0	0.98±12.29	0.915	151.0	72.4±30.9	72.2±30.6	0.25±1.84	0.998	3.39	44.6 (29.8-66.7)	<0.001
Vessel volume (mm ³)	135.8±58.4	134.6±56.6	1.17±21.65	0.929	468.7	139.4±58.8	139.0±58.7	0.44±2.82	0.999	7.95	59.0 (39.4-88.1)	<0.001
TAV (mm ³)	66.2±33.4	66.0±32.8	0.19±10.61	0.949	112.6	67.0±33.5	66.8±33.6	0.15±1.75	0.999	3.07	36.7 (24.5-54.9)	<0.001
PAV (%)	47.39±10.68	47.69±10.38	-0.30±2.07	0.980	4.27	46.81±10.47	46.77±10.46	0.04±0.87	0.997	0.76	5.62 (3.74-8.36)	<0.001

Table footnote: CI, confidence interval; ED, end-diastolic; ICC, intraclass correlation coefficient; PAV; percent atheroma volume; TAV, total atheroma volume.

* ICC and the variance of differences were used to compare the estimations of the 1st and 2nd analysis for the conventional and ED approach.

** The variance ratio was used to compare the reproducibility of the conventional and ED approach; a P<0.05 indicates statistically significant differences.

1
2
3
4
5
6
7

Supplementary Table 1. Comparison of the estimations of the conventional and the ED analysis for the normalised lumen, vessel, TAV and PAV in segments of interest with a fixed length.

	1 st 1mm analysis	2 nd 1mm analysis	Δ	ICC	Variance of differences	1 st ED analysis	2 nd ED analysis	Δ	ICC*	Variance of differences**	Variance ratio (95% CI)	P
Lumen volume (mm ³)	396.9±264.4	397.0±262.6	-0.14±9.13	0.999	83.4	406.2±268.9	405.4±268.7	0.76±4.03	1.000	16.2	5.15 (2.75-7.52)	<0.001
Vessel volume (mm ³)	646.8±427.9	648.9±429.3	-2.29±8.91	1.000	79.4	653.4±429.9	653.1±429.4	0.30±1.79	1.000	3.2	24.8 (16.6 - 37.1)	<0.001
TAV (mm ³)	249.8±174.5	251.9±176.9	-2.16±11.29	0.998	127.5	247.2±173.4	247.7±173.3	-0.46±4.03	1.000	16.2	7.87 (1.37-14.31)	<0.001
PAV (%)	38.04±7.75	38.17±7.71	-0.12±1.23	0.987	1.51	37.38±7.96	37.49±7.91	-0.12±0.59	0.997	0.35	4.31 (2.11 - 6.52)	<0.001

19
20
21
22
23
24
25
26
27
28
29
30
31
32
33
34
35
36
37
38
39
40
41
42
43
44
45
46

Table footnote: CI, confidence interval; ED, end-diastolic; ICC, intraclass correlation coefficient; PAV; percent atheroma volume; TAV, total atheroma volume.

* ICC and the variance of differences were used to compare the estimations of the 1st and 2nd analysis for the conventional and ED approach.

** The variance ratio was used to compare the reproducibility of the conventional and ED approach; a P<0.05 indicates statistically significant differences.

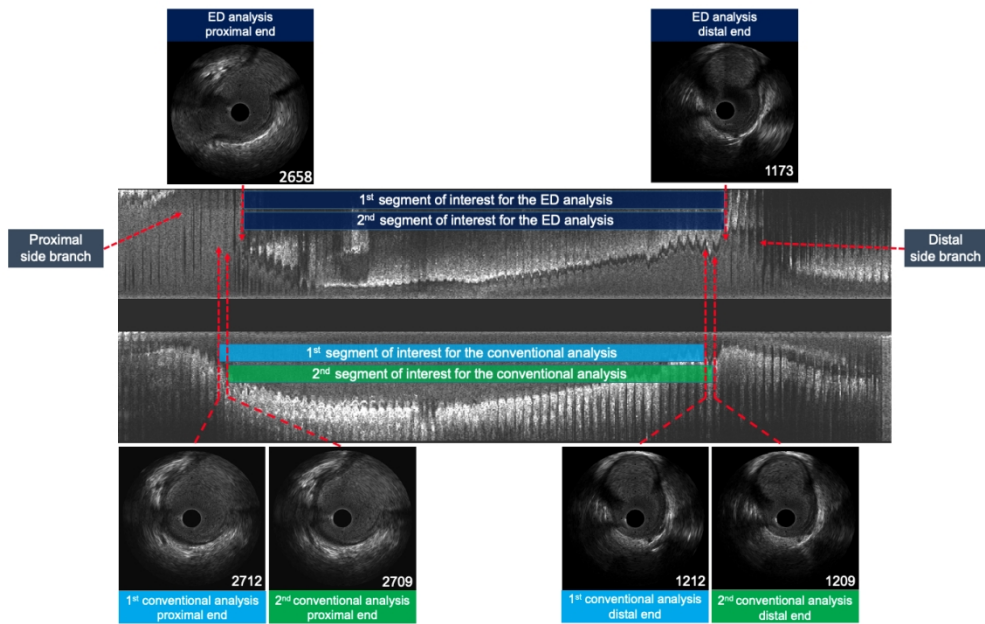


Figure 1. A case example showing the segment of interest defined by the conventional and the ED approach. In the ED approach, the proximal and distal end of the segment of interest coincide; conversely, in the conventional approach there was 3 frame difference between the estimations of the expert analyst for the location of the distal end of the segment of interest.

117x74mm (300 x 300 DPI)

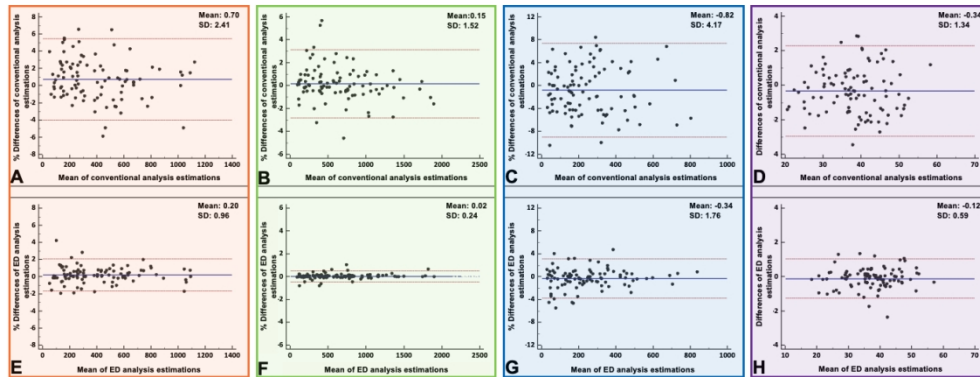
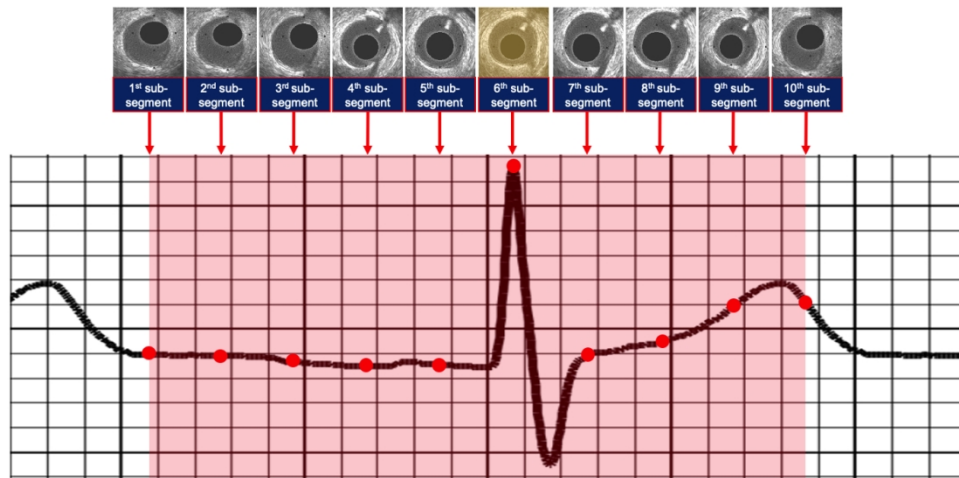


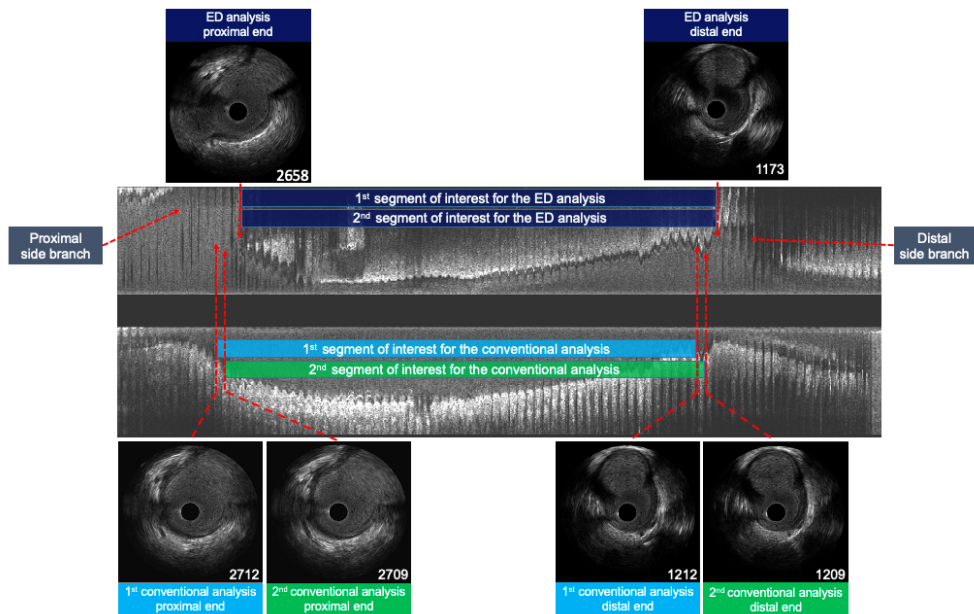
Figure 2. Bland-Altman plots of the % differences of the estimations of the expert analyst for the normalised lumen, vessel, TAV and the PAV in the conventional analysis (A, B, C and D respectively) and ED analysis (E, F, G and H respectively)

120x46mm (300 x 300 DPI)



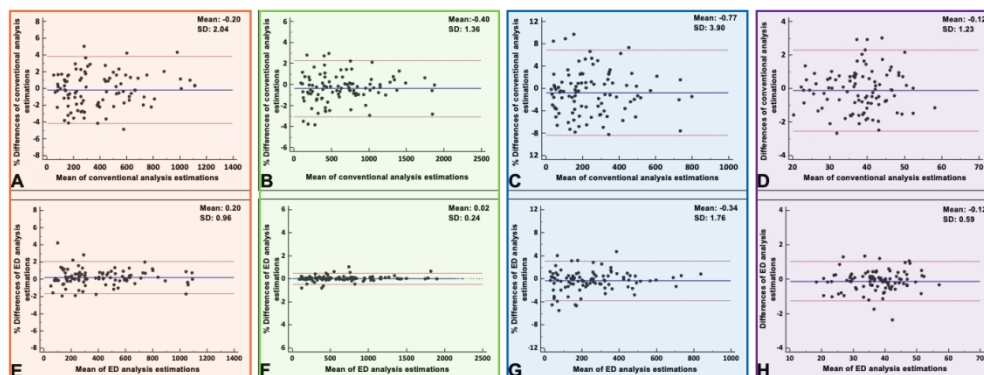
Supplementary Figure 1. Methodology applied to identify the 10 sub-segments that will be used to define the distal end of the segment of interest in the second fixed-length analysis using the conventional approach. After the detection of the most distal ED frame – i.e., the frame at the peak of the QRS complex – of the segment of interest using the DL methodology, then the cardiac cycle was split to 10 sub-segments; 5 sub-segments were defined distally and 4 proximally to the ED frame. One of these frames will be considered as the distal end of the segment of interest in the second fixed-length analysis using the conventional approach.

123x60mm (300 x 300 DPI)



Supplementary Figure 2. Segment of interest defined by the ED and the conventional approach in the fixed-length analysis. The distal end of the segment of interest was similar in the two ED analyses and the 1st conventional analysis. In the 2nd conventional analysis, the distal end of the segment of interest was located 3 frames more proximally – corresponding to the first sub-segment of the period between two end-diastolic frames.

87x54mm (300 x 300 DPI)



Supplementary Figure 3. Bland-Altman plots of the % differences of the estimations of the expert analyst for the normalised lumen, vessel, TAV and the PAV in the fixed-length analyses for the conventional (A, B, C and D respectively) and the ED approaches (E, F, G and H respectively).

119x45mm (300 x 300 DPI)

End-diastolic segmentation of intravascular ultrasound images enables more reproducible volumetric analysis of atheroma burden

Abstract

Background: Volumetric intravascular ultrasound (IVUS) analysis is currently performed at a fixed frame interval, neglecting the cyclic changes in vessel dimensions occurring during the cardiac cycle that can affect the reproducibility of the results. Analysis of end-diastolic (ED) IVUS frames has been proposed to overcome this limitation. However, at present, there is lack of data to support its superiority over conventional IVUS.

Objectives: The present study aims to compare the reproducibility of IVUS volumetric analysis performed at a fixed frame interval and at the ED frames, identified retrospectively using a novel deep-learning (DL) methodology.

Methods: IVUS data acquired from 97 vessels were included in the present study; each vessel was segmented at 1mm interval (conventional approach) and at ED frame twice by an expert analyst. Reproducibility was tested for the following metrics; normalised lumen, vessel and total atheroma volume (TAV) and percent atheroma volume (PAV).

Results: The mean length of the analysed segments was 50.0 ± 24.1 mm. ED analysis was more reproducible than the conventional analysis for the normalised lumen (mean difference: 0.76 ± 4.03 mm³ vs 1.72 ± 11.37 mm³; P for the variance of differences ratio <0.001), vessel (0.30 ± 1.79 mm³ vs -0.47 ± 10.26 mm³; P <0.001), TAV (-0.46 ± 4.03 mm³ vs -2.19 ± 14.39 mm³; P <0.001) and PAV ($-0.12 \pm 0.59\%$ vs $-0.34 \pm 1.34\%$; P <0.001). Results were similar when the analysis focused on the 10mm most diseased segment. The superiority of the ED approach was due to a more reproducible detection of the segment of interest and to the fact that it was not susceptible to the longitudinal motion of the IVUS probe and the cyclic changes in vessel dimensions during the cardiac cycle.

Conclusions: ED IVUS segmentation enables more reproducible volumetric analysis and quantification of TAV and PAV that are established end-points in longitudinal studies assessing the efficacy of novel pharmacotherapies. Therefore, it should be preferred over conventional IVUS analysis

1
2
3 as its higher reproducibility is expected to have an impact on the sample size calculation for the primary
4
5 end-point.
6

7 **Keywords:** Intravascular ultrasound; near-infrared spectroscopy; machine learning.
8
9
10
11
12
13
14
15
16
17
18
19
20
21
22
23
24
25
26
27
28
29
30
31
32
33
34
35
36
37
38
39
40
41
42
43
44
45
46
47
48
49
50
51
52
53
54
55
56
57
58
59
60

For Review Only

Introduction

Intravascular ultrasound (IVUS) imaging-based surrogate end-points have been traditionally used to examine the efficacy of novel pharmacotherapies in inhibiting atherosclerotic disease progression (1). Several studies over recent years have used serial IVUS imaging to investigate the role of emerging invasive and non-invasive therapies on vessel wall pathology and plaque evolution. In these reports, IVUS segmentation is traditionally performed at 1mm intervals without taking into account the phase of the cardiac cycle at which these frames are acquired (2-5). However, volumetric analysis with this approach is susceptible to the effect of the longitudinal motion of the IVUS catheter within the vessel and to changes in lumen dimensions during the cardiac cycle which can influence the reported results (6-9). Acknowledging these limitations, in the early days of IVUS, hardware were designed for electrocardiographic (ECG)-gated IVUS image acquisition, and software developed that enabled automated retrospective gating of the IVUS images, taking advantage of the lateral motion of the IVUS catheter in the lumen (10-13). However, these approaches have failed to have broad applications in research as ECG-gated IVUS image acquisition is a time-consuming process, while the developed algorithms for retrospective IVUS gating have not been robustly validated using ECG-estimations as a reference standard, or have not been incorporated in commercially available, user-friendly software. Moreover, there is a lack of data to indicate that IVUS-gated image analysis enables more reproducible quantification of atheroma burden than conventional IVUS segmentation at 1mm interval (14-16). We have recently introduced a novel deep-learning (DL) methodology that is capable of retrospectively detecting the end-diastolic (ED) frames in an IVUS sequence within 15s. The proposed methodology has been incorporated in a user-friendly IVUS-analysis software (QCU-CMS version 4.69; Leiden, University Medical Center, Leiden, The Netherlands), has been validated against ECG-estimations and it has been found to have an excellent accuracy in correctly detecting the ED frames (17). However, the value of this novel DL approach in enabling more reproducible IVUS volumetric analysis has not been explored yet.

Materials and Methods

Study population

1
2
3 We analysed IVUS sequences from patients recruited to the “Evaluation of the efficacy of computed
4 tomographic coronary angiography (CTCA) in assessing coronary artery morphology and physiology”
5 study (NCT03556644). The rationale and study design have been presented previously; in brief, 70
6 patients with stable angina that had obstructive disease on coronary angiography were considered for
7 inclusion. All the patients underwent computed tomography coronary angiography and then were listed
8 for 3-vessel near infrared spectroscopy (NIRS)-IVUS imaging and percutaneous coronary intervention
9 (18). The study protocol complied with the Declaration of Helsinki and was approved by the local
10 research ethics committee; all recruited patients gave written informed consent.
11
12
13
14
15
16
17
18
19
20
21

22 *NIRS-IVUS imaging and segment of interest selection*

23
24 NIRS-IVUS imaging was performed using the Dualpro system (Infraredx, Burlington, Massachusetts,
25 United States). After intracoronary administration of 400mcg nitrates, the NIRS-IVUS catheter was
26 advanced to the distal vessel and an angiographic projection was acquired under contrast dye injection
27 to identify its location within the vessel. Pullback was performed at a constant speed of 0.5mm/s using
28 an automated pullback device at a frame-rate of 30fps. The pullback was completed when the NIRS-
29 IVUS probe entered in the guide catheter. The acquired images were stored in DICOM format and
30 transferred to a workstation for further analysis.
31
32
33
34
35
36
37
38

39 Two interventional cardiologists (CB and AR) reviewed the angiographic images and identified native
40 non-angulated segments that were interrogated by NIRS-IVUS imaging for a length >20mm, exhibited
41 non-flow limiting coronary artery disease – assessed when it was deemed necessary with a fractional
42 flow reserve (FFR) study - and had a lesion/lesions with a maximum diameter stenosis of >20% (15).
43 Segments fulfilling the above criteria were included in the present analysis.
44
45
46
47
48
49
50
51

52 *Conventional versus ED analysis*

53 NIRS-IVUS analysis was performed by an expert analyst whose reproducibility was tested in 20 vessels
54 (supplementary file). Data analysis was performed using two different protocols. In the first, the
55 conventional approach, an expert analyst reviewed the NIRS-IVUS sequence and the angiographic runs
56 and identified the most proximal and distal side-branches that were visible in both NIRS-IVUS and
57
58
59
60

1
2
3 angiographic images to define the segment of interest. NIRS-IVUS segmentation started from a static
4 frame with no motion artifacts portraying the most proximal part of the distal side-branch and was
5 performed at 1mm intervals until the distal end of the proximal side-branch using the QCU-CMS
6 version 4.69 software (Figure 1). In these frames, the lumen and external elastic membrane (EEM)
7 borders were annotated according to the consensus document on the standards for IVUS imaging
8 analysis (15). To examine the reproducibility of this analysis, the identification of the proximal and
9 distal end of the segment of interest and the NIRS-IVUS segmentation was repeated by the same analyst
10 after a 2-month interval.
11

12
13 The second approach – the ED analysis – included the inspection of the angiographic and NIRS-IVUS
14 runs and the identification of the proximal and distal end of the segment of interest by the same operator
15 as before. Then, the DL methodology that has been incorporated into the QCU-CMS software and
16 described in the supplementary file was used to identify the ED NIRS-IVUS frames (17). Analysis was
17 performed from the last ED frame portraying the distal side-branch to the first ED frame portraying the
18 proximal side-branch (Figure 1). If the distal side-branch was not visible in the ED frames, then the
19 frame where the side-branch had its largest circumferential extent was identified and analysis started
20 from the first ED frame located after that frame. The same approach was used if the proximal side-
21 branch was not visible in the ED frames; the analysis was ended in the ED frame before the frame where
22 the side-branch had its largest circumferential extent. To evaluate the reproducibility of this analysis,
23 the expert analyst identified the proximal and distal end of the segment of interest and performed the
24 NIRS-IVUS segmentation twice within a 2-month interval.
25

26
27 The above validation methodology allows assessment of the reproducibility of the conventional and the
28 ED segmentation in IVUS volumetric analyses, but it is unclear whether variations in the estimated
29 volumes are due to differences in the length of the segment of interest or to the effect of the longitudinal
30 motion of the IVUS catheter and the changes in vessel dimensions occurring during the cardiac cycle.
31 To estimate the effect of the longitudinal motion of the catheter within the vessel and of the changes in
32 lumen dimensions on volume measurements, a fixed-length analysis was performed (supplementary
33 file).
34

35
36
37
38
39
40
41
42
43
44
45
46
47
48
49
50
51
52
53
54
55
56
57
58
59
60
Volumetric definitions

1
2
3 The lumen and EEM annotations were used to estimate metrics that have been extensively used in serial
4 intravascular imaging studies of atherosclerosis to examine the effect of novel pharmacotherapies in
5 atherosclerotic disease progression (15). More specially, for each segment of interest, the following
6 metrics were estimated: segment length, lumen volume, EEM volume, total atheroma volume (TAV)
7 and percent atheroma volume (PAV). To account for the differences in the length of the corresponding
8 segments of interest, the normalised lumen, EEM and TAV were estimated as previously described
9 (15). In addition, in each segment of interest, the most diseased 10mm segment – defined as the segment
10 with the largest PAV – was identified, and for this, the lumen, EEM, TAV and PAV were computed.
11
12
13
14
15
16
17
18
19
20
21

22 **Sample size calculation and statistical analysis**

23
24 The study of Jensen et al. is the only report that examined the reproducibility of IVUS segmentation
25 using the conventional 1mm analysis and a prospective ECG-gated pullback approach (14). In this study
26 the mean±standard deviation (SD) of the PAV estimations between the first and second segmentation
27 was $-0.94\pm 3.93\%$ for the conventional and $0.2\pm 3.25\%$ for the ECG-gated analysis. Assuming that in
28 our study the SD for the differences between the first and second segmentation will be 4% for the PAV
29 in the conventional analysis and 3% in the ED analysis, we estimated that we need to include 97
30 segments to prove with a power of 80% and an alpha of 0.05 that ED approach is more reproducible
31 than the conventional approach.
32
33
34
35
36
37
38
39
40

41 Continuous variables are presented as mean±SD, while categorical variables as absolute numbers and
42 percentages. Kolmogorov-Smirnov test was used to examine the distribution of continuous variables; a
43 non-normal distribution was found, and therefore, comparisons between these variables were performed
44 using the Mann Whitney U test, while categorical variables were compared using the chi-square or
45 Fisher's exact test. Bland-Altman analysis, intraclass correlation coefficient (ICC) and variance of
46 difference were used to compare the intra-observer variability in the conventional and ED approach,
47 while the variance ratio was used to compare the reproducibility of the expert between the two
48 approaches. Significance was tested using a robust test for the equality of variances (Brown and
49 Forsythe test). The confidence interval of the variance ratio was estimated using bootstrap re-sampling
50
51
52
53
54
55
56
57
58
59
60

1
2
3 in 1000 samples. Analysis was performed using Stata version 16 (StataCorp, Texas); a P-value <0.05
4
5 was considered statistically significant.
6
7
8

9 **Results**

10 *Studied population*

11
12 Data from 55 out of the 70 patients recruited in the study were included in the present analysis. The
13
14 baseline demographics of the patients and analysed vessels are shown in Table 1. Most of the patients
15
16 were males, had a family history of coronary artery disease, suffered from hypercholesterolemia and
17
18 were in sinus rhythm. The average heart rate was 64 ± 7 (range: 48-78) beats per minute; there was a
19
20 balanced representation of the three coronary arteries in the analysis.
21
22
23
24
25

26 *Conventional versus ED approach*

27
28 The mean length of the analysed segments was 49.96 ± 24.00 mm. In the conventional analyses, the first
29
30 frame of the segment of interest coincided in only 6.19% of the cases, while in the ED analyses in all
31
32 cases. The mean distance difference between the location of the first analysed frame in the two
33
34 conventional analyses was 0.19 ± 0.22 mm, whereas in the ED approach the first frame of the segment of
35
36 interest coincided in all the analyses. The different location of the first frame had an impact on the
37
38 length of the analysed segments; the mean length difference between first and second segmentation in
39
40 the conventional approach was significantly larger than the length difference noted in the ED approach
41
42 (Table 2). The ICC was close to 1 in all the volumetric analyses; however, a larger intra-observer
43
44 variability was noted between the estimations of the expert analyst – as indicated by the variance ratio
45
46 – for the normalised lumen and vessel volumes, TAV and the PAV in the conventional than the ED
47
48 approach (Table 2, Figure 2).
49

50
51 Results were similar for the fixed-length analysis (supplementary file, Table 1, and Figure 3) and when
52
53 the analysis focused on the 10mm most diseased segment. As before, the distance difference between
54
55 the first frame of the most diseased 10mm segment was significantly larger in the conventional than the
56
57 ED analyses (4.96 ± 11.83 mm vs 0.65 ± 4.63 mm, $P<0.001$). The different location of the most diseased
58
59 10mm segment in the two conventional analyses resulted in large differences for the estimated lumen
60

1
2
3 and vessel volumes, TAV and PAV (Table 2). Conversely, in the ED approach, where the location of
4 the 10mm segment coincided in most of the cases, the intra-observer agreement was high for the
5 measured volumes (Table 2).
6
7
8
9

10 11 **Discussion**

12
13 The present study, for the first time, examined the value of a recently introduced DL methodology that
14 allows retrospective identification of ED frames, for improvement of the reproducibility of IVUS
15 volumetric analysis in native coronary arteries. We demonstrated 1) a high intra-observer agreement
16 for normalised lumen and vessel volumes, as well as the TAV and PAV, that have been extensively
17 used as primary end-points in serial IVUS-based studies assessing the efficacy of novel
18 pharmacotherapies on plaque evolution – in the ED approach that is superior to the conventional
19 approach; 2) that these results were consistent when analysis focused on the 10mm most diseased
20 segment which often constitutes a secondary end-point of serial intravascular imaging studies
21 examining the efficacy of emerging therapies in inhibiting plaque evolution, and 3) that the improved
22 reproducibility of the ED analysis is due not only to the fact that it overcomes the errors induced by the
23 longitudinal motion of the IVUS catheter and the changes in the lumen dimensions during the cardiac
24 cycle but also to its superior reproducibility in identifying the segment of interest compared to the
25 conventional approach.
26
27
28
29
30
31
32
33
34
35
36
37
38
39
40

41 Cumulative evidence from the early days of IVUS imaging have demonstrated significant changes in
42 the lumen and vessel dimensions during the cardiac cycle. Ge et al. were the first that systematically
43 examined the changes in the left main stem and left anterior descending artery reporting a pulsatile
44 variation in the lumen cross-sectional area of 10% (8). These results were also confirmed by the study
45 of Weismann et al. who included all the three epicardial coronary arteries and reported an average
46 change in lumen, vessel and plaque area of 8.1%, 3.7% and 4.9% respectively (7). These changes were
47 more prominent in disease-free segments and in segments with non-calcified plaques compared to IVUS
48 frames portraying calcific-rich plaques.
49
50
51
52
53
54
55
56

57 In addition, studies have shown that there is a longitudinal motion of the IVUS probe with regards to
58 the vessel during the cardiac cycle. Arab Zaden et al. have estimated an average longitudinal motion of
59
60

1
2
3 the IVUS probe during the cardiac cycle of 1.50 ± 0.80 mm (range 0.5-5.5mm); while Talou et al.
4 confirmed these findings and showed that the longitudinal motion of the IVUS probe varies depending
5 on the studied vessel (6,9).
6
7

8
9 Therefore, it has been speculated that non-gated IVUS analysis, which neglects the cyclic changes in
10 vessel dimensions and the longitudinal motion of the IVUS catheter within the vessel, has a limited
11 reproducibility in assessing PAV (19). However, this hypothesis was not confirmed by the study of
12 Jensen et al. – the only report that compared the reproducibility of IVUS-gated and non-gated
13 segmentation and reported similar intra-observer agreement. A possible explanation of this paradox is
14 the fact that the study was underpowered in detecting statistically significant differences between the
15 two analyses as it included only 19 coronary artery segments (14). In view of these findings, the current
16 recommendation is to analyse IVUS imaging data neglecting the phase of the cardiac cycle at which
17 these images were acquired (15).
18
19

20
21 The present study examined for the first time the value of ED IVUS segmentation, using a newly
22 developed DL methodology for retrospective ED frame detection, in improving the reproducibility of
23 IVUS analysis. We included an appropriately-powered sample size of 97 vessels that were analysed by
24 an expert analyst twice and demonstrated that the ED analysis improves the intra-observer agreement
25 of the expert for the quantification of the normalised lumen, vessel, TAV and PAV. This was attributed
26 to the higher agreement of the ED analyses for the proximal and distal end of the segment of interest
27 that determine its length but also to the longitudinal displacement of the IVUS probe and the cyclic
28 changes in vessel areas during the cardiac cycle as it was demonstrated in the fixed-length analysis. The
29 value of ED approach was more prominent in the quantification of the TAV and PAV in the 10mm
30 most diseased segment, as the conventional approach had a weak reproducibility in identifying its
31 location in the segment of interest.
32
33

34
35 IVUS imaging has been extensively used over the recent years to assess the effect of novel therapies on
36 PAV and provide mechanistic insights about their implications on plaque morphology (1). In these
37 studies, established pharmacotherapies which appeared effective in improving clinical outcomes had a
38 marginal but consistent effect on PAV, resulting in a PAV reduction that ranged from 0.3-1.4% (2,4,20-
39 22). In this setting, IVUS segmentation is essential to be reproducible as the reliability of a change in
40
41
42
43
44
45
46
47
48
49
50
51
52
53
54
55
56
57
58
59
60

1
2
3 PAV will compound error from both measures, impacting on the required sample size. For example,
4 the observed ICC for the PAV of 0.997 for the ED approach and of 0.985 for the conventional approach
5 would reduce to 0.973 and 0.864 for the change in PAV if we assume that the correlation for the PAV
6 between baseline and follow-up IVUS examinations is 0.89 (23,24); this would result in an 11%
7 reduction in the required sample size by using the more reliable measurement (25). Therefore, in order
8 to detect a 1% reduction in the PAV with an 80% power and 5% alpha, we would need to recruit 111
9 patients if the SD is 1.34% for baseline and follow-up measures and the ICC for PAV is 0.985 – as it
10 was reported in our study with the conventional approach – and 100 patients if the ICC for the PAV
11 improves to 0.997 and the SD to 0.59 with the use of an ED approach. Thus, ED analysis should be
12 considered in serial IVUS-based imaging studies as reducing the sample size is anticipated to decrease
13 their cost and expedite patient recruitment.
14
15

16 The accurate and reproducible quantification of atherosclerotic disease severity using the ED analysis
17 is also likely to enable more accurate estimation of the FFR using IVUS-based computational modelling
18 (26,27). However, this has to be proven in a prospective, appropriately powered clinical study.
19
20

21 *Limitations*

22 A major limitation of the present study is the fact we tested the reproducibility of the volumetric
23 analyses in IVUS sequences acquired at one time-point and not in sequential IVUS examinations
24 performed during the index procedure as it has been reported in previous analyses (14,28). It is apparent
25 however that the latter would have been possible only in the context of a prospective, large-scale clinical
26 study with pre-specified imaging end-points. Moreover, we did not test the reproducibility of the two
27 approaches to assess changes in the PAV in patients who had IVUS imaging at baseline and after
28 treatment with medications that inhibit atherosclerotic evolution. In addition, the ED analysis is feasible
29 only for IVUS data acquired by a catheter that is withdrawn at low speed as high-speed IVUS pullbacks
30 would result in acquisition of only a handful of end-diastolic IVUS frames per segment. Furthermore,
31 the study was performed using a high-resolution IVUS system so it is unclear whether the reported
32 results would apply to IVUS data acquired by 20MHz or 40MHz IVUS catheters. Moreover, the DL
33 methodology was developed to detect ED frames in patients in sinus rhythm and was tested in this study
34 in a population that was predominantly in sinus rhythm. Further research is needed to examine its
35
36
37
38
39
40
41
42
43
44
45
46
47
48
49
50
51
52
53
54
55
56
57
58
59
60

1
2
3 performance in patients with atrial fibrillation and its value in improving the reproducibility of IVUS
4
5 segmentation in this population.
6
7
8

9 **Conclusions**

10 ED IVUS segmentation enables more reproducible IVUS volumetric analysis allowing accurate
11
12 quantification of the normalised lumen, vessel, TAV and the PAV, compared to the conventional
13
14 approach which is currently used by most core-labs. The superiority of ED analysis should be attributed
15
16 to the higher intra-observer agreement in defining the segment of interest but also to the fact that is not
17
18 susceptible to the longitudinal motion of the IVUS catheter and the cyclic changes in vessel dimensions
19
20 during the cardiac cycle. Therefore, the ED approach should be preferred over the conventional
21
22 approach for the analysis of IVUS data acquired in longitudinal studies assessing the efficacy of focal
23
24 and systemic therapies targeting atherosclerosis.
25
26
27
28
29
30
31
32

33 **Data Availability Statement**

34 Data is readily available upon request
35
36
37
38
39
40
41
42
43
44
45
46
47
48
49
50
51
52
53
54
55
56
57
58
59
60

References

1. Bose D, von Birgelen C, Erbel R. Intravascular ultrasound for the evaluation of therapies targeting coronary atherosclerosis. *J Am Coll Cardiol* 2007;49(9):925-32.
2. Nicholls SJ, Ballantyne CM, Barter PJ, Chapman MJ, Erbel RM, Libby P, Raichlen JS, Uno K, Borgman M, Wolski K and others. Effect of two intensive statin regimens on progression of coronary disease. *N Engl J Med* 2011;365(22):2078-87.
3. Nissen SE, Tuzcu EM, Schoenhagen P, Brown BG, Ganz P, Vogel RA, Crowe T, Howard G, Cooper CJ, Brodie B and others. Effect of intensive compared with moderate lipid-lowering therapy on progression of coronary atherosclerosis: a randomized controlled trial. *JAMA* 2004;291(9):1071-80.
4. Nissen SE, Nicholls SJ, Sipahi I, Libby P, Raichlen JS, Ballantyne CM, Davignon J, Erbel R, Fruchart JC, Tardif JC and others. Effect of very high-intensity statin therapy on regression of coronary atherosclerosis: the ASTEROID trial. *JAMA* 2006;295(13):1556-65.
5. Tardif JC, Gregoire J, L'Allier PL, Ibrahim R, Lesperance J, Heinonen TM, Kouz S, Berry C, Basser R, Lavoie MA and others. Effects of reconstituted high-density lipoprotein infusions on coronary atherosclerosis: a randomized controlled trial. *JAMA* 2007;297(15):1675-82.
6. Arbab-Zadeh A, DeMaria AN, Penny WF, Russo RJ, Kimura BJ, Bhargava V. Axial movement of the intravascular ultrasound probe during the cardiac cycle: implications for three-dimensional reconstruction and measurements of coronary dimensions. *Am Heart J* 1999;138(5 Pt 1):865-72.
7. Weissman NJ, Palacios IF, Weyman AE. Dynamic expansion of the coronary arteries: implications for intravascular ultrasound measurements. *Am Heart J* 1995;130(1):46-51.
8. Ge J, Erbel R, Gerber T, Gorge G, Koch L, Haude M, Meyer J. Intravascular ultrasound imaging of angiographically normal coronary arteries: a prospective study in vivo. *Br Heart J* 1994;71(6):572-8.

- 1
2
3 9. Talou GD, Blanco PJ, Larrabide I, Bezerra CG, Lemos PA, Feijoo RA. Registration Methods
4 for IVUS: Transversal and Longitudinal Transducer Motion Compensation. *IEEE Trans*
5 *Biomed Eng* 2017;64(4):890-903.
6
7
- 8
9
10 10. von Birgelen C, de Vrey EA, Mintz GS, Nicosia A, Bruining N, Li W, Slager CJ, Roelandt JR,
11 Serruys PW, de Feyter PJ. ECG-gated three-dimensional intravascular ultrasound: feasibility
12 and reproducibility of the automated analysis of coronary lumen and atherosclerotic plaque
13 dimensions in humans. *Circulation* 1997;96(9):2944-52.
14
15
- 16
17
18 11. De Winter SA, Hamers R, Degertekin M, Tanabe K, Lemos PA, Serruys PW, Roelandt JR,
19 Bruining N. Retrospective image-based gating of intracoronary ultrasound images for improved
20 quantitative analysis: the intelligate method. *Catheter Cardiovasc Interv* 2004;61(1):84-94.
21
22
- 23
24 12. Maso Talou GD, Larrabide I, Blanco PJ, Bezerra CG, Lemos PA, Feijoo RA. Improving
25 Cardiac Phase Extraction in IVUS Studies by Integration of Gating Methods. *IEEE Trans*
26 *Biomed Eng* 2015;62(12):2867-77.
27
28
- 29
30 13. Torbati N, Ayatollahi A, Sadeghipour P. Image-Based Gating of Intravascular Ultrasound
31 Sequences Using the Phase Information of Dual-Tree Complex Wavelet Transform
32 Coefficients. *IEEE Trans Med Imaging* 2019;38(12):2785-2795.
33
34
- 35
36
37 14. Jensen LO, Thayssen P. Accuracy of electrocardiographic-gated versus nongated volumetric
38 intravascular ultrasound measurements of coronary arterial narrowing. *Am J Cardiol*
39 2007;99(2):279-83.
40
41
- 42
43 15. Mintz GS, Garcia-Garcia HM, Nicholls SJ, Weissman NJ, Bruining N, Crowe T, Tardif JC,
44 Serruys PW. Clinical expert consensus document on standards for acquisition, measurement
45 and reporting of intravascular ultrasound regression/progression studies. *EuroIntervention*
46 2011;6(9):1123-30, 9.
47
48
- 49
50
51 16. Gerstein HC, Ratner RE, Cannon CP, Serruys PW, Garcia-Garcia HM, van Es GA, Kolatkar
52 NS, Kravitz BG, Miller DM, Huang C and others. Effect of rosiglitazone on progression of
53 coronary atherosclerosis in patients with type 2 diabetes mellitus and coronary artery disease:
54 the assessment on the prevention of progression by rosiglitazone on atherosclerosis in diabetes
55 patients with cardiovascular history trial. *Circulation* 2010;121(10):1176-87.
56
57
58
59
60

17. Bajaj R, Huang X, Kilic Y, Jain A, Ramasamy A, Torii R, Moon J, Koh T, Crake T, Parker MK and others. A deep learning methodology for the automated detection of end-diastolic frames in intravascular ultrasound images *Int J Cardiovasc Imaging*. 2021.
18. Ramasamy A, Safi H, Moon JC, Andiapen M, Rathod KS, Maurovich-Horvat P, Bajaj R, Serruys PW, Mathur A, Baumbach A and others. Evaluation of the Efficacy of Computed Tomographic Coronary Angiography in Assessing Coronary Artery Morphology and Physiology: Rationale and Study Design. *Cardiology* 2020;145(5):285-293.
19. De Winter SA, Hamers R, Roelandt JR, Serruys PW, Bruining N. Quantitative gated intravascular ultrasound largely reduces the population size for atherosclerosis progression-regression trials: a computer simulation study. 36th Annual Computers in Cardiology Conference; Park City, UT 2009:829-832.
20. Raber L, Taniwaki M, Zaugg S, Kelbaek H, Roffi M, Holmvang L, Noble S, Pedrazzini G, Moschovitis A, Luscher TF and others. Effect of high-intensity statin therapy on atherosclerosis in non-infarct-related coronary arteries (IBIS-4): a serial intravascular ultrasonography study. *Eur Heart J* 2015;36(8):490-500.
21. Tsujita K, Sugiyama S, Sumida H, Shimomura H, Yamashita T, Yamanaga K, Komura N, Sakamoto K, Oka H, Nakao K and others. Impact of Dual Lipid-Lowering Strategy With Ezetimibe and Atorvastatin on Coronary Plaque Regression in Patients With Percutaneous Coronary Intervention: The Multicenter Randomized Controlled PRECISE-IVUS Trial. *J Am Coll Cardiol* 2015;66(5):495-507.
22. Nicholls SJ, Puri R, Anderson T, Ballantyne CM, Cho L, Kastelein JJ, Koenig W, Somaratne R, Kassahun H, Yang J and others. Effect of Evolocumab on Progression of Coronary Disease in Statin-Treated Patients: The GLAGOV Randomized Clinical Trial. *JAMA* 2016;316(22):2373-2384.
23. Nissen SE, Tuzcu EM, Libby P, Thompson PD, Ghali M, Garza D, Berman L, Shi H, Buebendorf E, Topol EJ and others. Effect of antihypertensive agents on cardiovascular events in patients with coronary disease and normal blood pressure: the CAMELOT study: a randomized controlled trial. *JAMA* 2004;292(18):2217-25.

- 1
2
3 24. May K, Hittner JB. On the relation between power and reliability of difference scores. *Percept*
4 *Mot Skills* 2003;97(3 Pt 1):905-8.
5
6
7 25. Perkins DO, Wyatt RJ, Bartko JJ. Penny-wise and pound-foolish: the impact of measurement
8 error on sample size requirements in clinical trials. *Biol Psychiatry* 2000;47(8):762-6.
9
10
11 26. Yu W, Tanigaki T, Ding D, Wu P, Du H, Ling L, Huang B, Li G, Yang W, Zhang S and others.
12 Accuracy of Intravascular Ultrasound-Based Fractional Flow Reserve in Identifying
13 Hemodynamic Significance of Coronary Stenosis. *Circ Cardiovasc Interv* 2021;14(2):e009840.
14
15
16 27. Sakurai S, Takashima H, Waseda K, Gosho M, Kurita A, Ando H, Maeda K, Suzuki A,
17 Fujimoto M, Amano T. Influence of plaque characteristics on fractional flow reserve for
18 coronary lesions with intermediate to obstructive stenosis: insights from integrated-backscatter
19 intravascular ultrasound analysis. *Int J Cardiovasc Imaging* 2015;31(7):1295-301.
20
21
22
23
24
25
26 28. Rodriguez-Granillo GA, Vaina S, Garcia-Garcia HM, Valgimigli M, Duckers E, van Geuns RJ,
27 Regar E, van der Giessen WJ, Bressers M, Goedhart D and others. Reproducibility of
28 intravascular ultrasound radiofrequency data analysis: implications for the design of
29 longitudinal studies. *Int J Cardiovasc Imaging* 2006;22(5):621-31.
30
31
32
33
34
35
36
37
38
39
40
41
42
43
44
45
46
47
48
49
50
51
52
53
54
55
56
57
58
59
60

Figure legends

Figure 1. A case example showing the segment of interest defined by the conventional and the ED approach. In the ED approach, the proximal and distal end of the segment of interest coincide; conversely, in the conventional approach there was 3 frame difference between the estimations of the expert analyst for the location of the distal end of the segment of interest.

Figure 2. Bland-Altman plots of the % differences of the estimations of the expert analyst for the normalised lumen, vessel, TAV and the PAV in the conventional analysis (A, B, C and D respectively) and ED analysis (E, F, G and H respectively).

Supplementary Figure 1. Methodology applied to identify the 10 sub-segments that will be used to define the distal end of the segment of interest in the second fixed-length analysis using the conventional approach. After the detection of the most distal ED frame – i.e., the frame at the peak of the QRS complex – of the segment of interest using the DL methodology, then the cardiac cycle was split to 10 sub-segments; 5 sub-segments were defined distally and 4 proximally to the ED frame. One of these frames will be considered as the distal end of the segment of interest in the second fixed-length analysis using the conventional approach.

Supplementary Figure 2. Segment of interest defined by the ED and the conventional approach in the fixed-length analysis. The distal end of the segment of interest was similar in the two ED analyses and the 1st conventional analysis. In the 2nd conventional analysis, the distal end of the segment of interest was located 3 frames more proximally – corresponding to the first sub-segment of the period between two end-diastolic frames.

Supplementary Figure 3. Bland-Altman plots of the % differences of the estimations of the expert analyst for the normalised lumen, vessel, TAV and the PAV in the fixed-length analyses for the conventional (A, B, C and D respectively) and the ED approaches (E, F, G and H respectively).

End-diastolic segmentation of intravascular ultrasound images enables more reproducible volumetric analysis of atheroma burden

Abstract

Background: Volumetric intravascular ultrasound (IVUS) analysis is currently performed at a fixed frame interval, neglecting the cyclic changes in vessel dimensions occurring during the cardiac cycle that can affect the reproducibility of the results. Analysis of end-diastolic (ED) IVUS frames has been proposed to overcome this limitation. However, at present, there is lack of data to support its superiority over conventional IVUS.

Objectives: The present study aims to compare the reproducibility of IVUS volumetric analysis performed at a fixed frame interval and at the ED frames, identified retrospectively using a novel deep-learning (DL) methodology.

Methods: IVUS data acquired from 97 vessels were included in the present study; each vessel was segmented at 1mm interval (conventional approach) and at ED frame twice by an expert analyst. Reproducibility was tested for the following metrics; normalised lumen, vessel and total atheroma volume (TAV) and percent atheroma volume (PAV).

Results: The mean length of the analysed segments was 50.0 ± 24.1 mm. **ED analysis** was more reproducible than the conventional analysis for the normalised lumen (mean difference: 0.76 ± 4.03 mm³ vs 1.72 ± 11.37 mm³; P for the variance of differences ratio <0.001), vessel (0.30 ± 1.79 mm³ vs -0.47 ± 10.26 mm³; P <0.001), TAV (-0.46 ± 4.03 mm³ vs -2.19 ± 14.39 mm³; P <0.001) and PAV ($-0.12 \pm 0.59\%$ vs $-0.34 \pm 1.34\%$; P <0.001). Results were similar when the analysis focused on the 10mm most diseased segment. The superiority of the **ED approach** was due to a more reproducible detection of the segment of interest and to the fact that it was not susceptible to the longitudinal motion of the IVUS probe and the cyclic changes in vessel dimensions during the cardiac cycle.

Conclusions: **ED** IVUS segmentation enables more reproducible volumetric analysis and quantification of TAV and PAV that are established end-points in longitudinal studies assessing the efficacy of novel pharmacotherapies. Therefore, it should be preferred over conventional IVUS analysis

1
2
3 as its higher reproducibility is expected to have an impact on the sample size calculation for the primary
4
5 end-point.
6

7 **Keywords:** Intravascular ultrasound; near-infrared spectroscopy; machine learning.
8
9
10
11
12
13
14
15
16
17
18
19
20
21
22
23
24
25
26
27
28
29
30
31
32
33
34
35
36
37
38
39
40
41
42
43
44
45
46
47
48
49
50
51
52
53
54
55
56
57
58
59
60

For Review Only

Introduction

Intravascular ultrasound (IVUS) imaging-based surrogate end-points have been traditionally used to examine the efficacy of novel pharmacotherapies in inhibiting atherosclerotic disease progression (1). Several studies over recent years have used serial IVUS imaging to investigate the role of emerging invasive and non-invasive therapies on vessel wall pathology and plaque evolution. In these reports, IVUS segmentation is traditionally performed at 1mm intervals without taking into account the phase of the cardiac cycle at which these frames are acquired (2-5). However, volumetric analysis with this approach is susceptible to the effect of the longitudinal motion of the IVUS catheter within the vessel and to changes in lumen dimensions during the cardiac cycle which can influence the reported results (6-9). Acknowledging these limitations, in the early days of IVUS, hardware were designed for electrocardiographic (ECG)-gated IVUS image acquisition, and software developed that enabled automated retrospective gating of the IVUS images, taking advantage of the lateral motion of the IVUS catheter in the lumen (10-13). However, these approaches have failed to have broad applications in research as ECG-gated IVUS image acquisition is a time-consuming process, while the developed algorithms for retrospective IVUS gating have not been robustly validated using ECG-estimations as a reference standard, or have not been incorporated in commercially available, user-friendly software. Moreover, there is a lack of data to indicate that IVUS-gated image analysis enables more reproducible quantification of atheroma burden than conventional IVUS segmentation at 1mm interval (14-16). We have recently introduced a novel deep-learning (DL) methodology that is capable of retrospectively detecting the end-diastolic (ED) frames in an IVUS sequence within 15s. The proposed methodology has been incorporated in a user-friendly IVUS-analysis software (QCU-CMS version 4.69; Leiden, University Medical Center, Leiden, The Netherlands), has been validated against ECG-estimations and it has been found to have an excellent accuracy in correctly detecting the ED frames (17). However, the value of this novel DL approach in enabling more reproducible IVUS volumetric analysis has not been explored yet.

Materials and Methods

Study population

1
2
3 We analysed IVUS sequences from patients recruited to the “Evaluation of the efficacy of computed
4 tomographic coronary angiography (CTCA) in assessing coronary artery morphology and physiology”
5 study (NCT03556644). The rationale and study design have been presented previously; in brief, 70
6 patients with stable angina that had obstructive disease on coronary angiography were considered for
7 inclusion. All the patients underwent computed tomography coronary angiography and then were listed
8 for 3-vessel near infrared spectroscopy (NIRS)-IVUS imaging and percutaneous coronary intervention
9 (18). The study protocol complied with the Declaration of Helsinki and was approved by the local
10 research ethics committee; all recruited patients gave written informed consent.
11
12
13
14
15
16
17
18
19
20
21

22 *NIRS-IVUS imaging and segment of interest selection*

23
24 NIRS-IVUS imaging was performed using the Dualpro system (Infraredx, Burlington, Massachusetts,
25 United States). After intracoronary administration of 400mcg nitrates, the NIRS-IVUS catheter was
26 advanced to the distal vessel and an angiographic projection was acquired under contrast dye injection
27 to identify its location within the vessel. Pullback was performed at a constant speed of 0.5mm/s using
28 an automated pullback device at a frame-rate of 30fps. The pullback was completed when the NIRS-
29 IVUS probe entered in the guide catheter. The acquired images were stored in DICOM format and
30 transferred to a workstation for further analysis.
31
32
33
34
35
36
37
38

39 Two interventional cardiologists (CB and AR) reviewed the angiographic images and identified native
40 non-angulated segments that were interrogated by NIRS-IVUS imaging for a length >20mm, exhibited
41 non-flow limiting coronary artery disease – assessed when it was deemed necessary with a fractional
42 flow reserve (FFR) study - and had a lesion/lesions with a maximum diameter stenosis of >20% (15).
43 Segments fulfilling the above criteria were included in the present analysis.
44
45
46
47
48
49
50
51

52 *Conventional versus ED analysis*

53 **NIRS-IVUS analysis was performed by an expert analyst whose reproducibility was tested in 20 vessels**
54 **(supplementary file).** Data analysis was performed using two different protocols. In the first, the
55 conventional approach, an expert analyst reviewed the NIRS-IVUS sequence and the angiographic runs
56 and identified the most proximal and distal side-branches that were visible in both NIRS-IVUS and
57
58
59
60

1
2
3 angiographic images to define the segment of interest. NIRS-IVUS segmentation started from a static
4 frame with no motion artifacts portraying the most proximal part of the distal side-branch and was
5 performed at 1mm intervals until the distal end of the proximal side-branch using the QCU-CMS
6 version 4.69 software (Figure 1). In these frames, the lumen and external elastic membrane (EEM)
7 borders were annotated according to the consensus document on the standards for IVUS imaging
8 analysis (15). To examine the reproducibility of this analysis, the identification of the proximal and
9 distal end of the segment of interest and the NIRS-IVUS segmentation was repeated by the same analyst
10 after a 2-month interval.

11
12 The second approach – the **ED analysis** – included the inspection of the angiographic and NIRS-IVUS
13 runs and the identification of the proximal and distal end of the segment of interest by the same operator
14 as before. Then, the DL methodology that has been incorporated into the QCU-CMS software and
15 described in the supplementary file was used to identify the ED NIRS-IVUS frames (17). **Analysis was**
16 **performed from the last ED frame portraying the distal side-branch to the first ED frame portraying the**
17 **proximal side-branch (Figure 1). If the distal side-branch was not visible in the ED frames, then the**
18 **frame where the side-branch had its largest circumferential extent was identified and analysis started**
19 **from the first ED frame located after that frame. The same approach was used if the proximal side-**
20 **branch was not visible in the ED frames; the analysis was ended in the ED frame before the frame where**
21 **the side-branch had its largest circumferential extent.** To evaluate the reproducibility of this analysis,
22 the expert analyst identified the proximal and distal end of the segment of interest and performed the
23 NIRS-IVUS segmentation twice within a 2-month interval.

24
25 The above validation methodology allows assessment of the reproducibility of the conventional and the
26 ED segmentation in IVUS volumetric analyses, but it is unclear whether variations in the estimated
27 volumes are due to differences in the length of the segment of interest or to the effect of the longitudinal
28 motion of the IVUS catheter and the changes in vessel dimensions occurring during the cardiac cycle.
29 To estimate the effect of the longitudinal motion of the catheter within the vessel and of the changes in
30 lumen dimensions on volume measurements, a fixed-length analysis was performed (**supplementary**
31 **file**).

32
33 *Volumetric definitions*

1
2
3 The lumen and EEM annotations were used to estimate metrics that have been extensively used in serial
4 intravascular imaging studies of atherosclerosis to examine the effect of novel pharmacotherapies in
5 atherosclerotic disease progression (15). More specially, for each segment of interest, the following
6 metrics were estimated: segment length, lumen volume, EEM volume, total atheroma volume (TAV)
7 and percent atheroma volume (PAV). To account for the differences in the length of the corresponding
8 segments of interest, the normalised lumen, EEM and TAV were estimated as previously described
9 (15). In addition, in each segment of interest, the most diseased 10mm segment – defined as the segment
10 with the largest PAV – was identified, and for this, the lumen, EEM, TAV and PAV were computed.
11
12
13
14
15
16
17
18
19
20
21

22 **Sample size calculation and statistical analysis**

23
24 The study of Jensen et al. is the only report that examined the reproducibility of IVUS segmentation
25 using the conventional 1mm analysis and a prospective ECG-gated pullback approach (14). In this study
26 the mean±standard deviation (SD) of the PAV estimations between the first and second segmentation
27 was $-0.94\pm 3.93\%$ for the conventional and $0.2\pm 3.25\%$ for the ECG-gated analysis. Assuming that in
28 our study the SD for the differences between the first and second segmentation will be 4% for the PAV
29 in the conventional analysis and 3% in the **ED analysis**, we estimated that we need to include 97
30 segments to prove with a power of 80% and an alpha of 0.05 that **ED approach** is more reproducible
31 than the conventional approach.
32
33
34
35
36
37
38
39
40

41 Continuous variables are presented as mean±SD, while categorical variables as absolute numbers and
42 percentages. Kolmogorov-Smirnov test was used to examine the distribution of continuous variables; a
43 non-normal distribution was found, and therefore, comparisons between these variables were performed
44 using the Mann Whitney U test, while categorical variables were compared using the chi-square or
45 Fisher's exact test. Bland-Altman analysis, intraclass correlation coefficient (ICC) and variance of
46 difference were used to compare the intra-observer variability in the conventional and **ED approach**,
47 while the variance ratio was used to compare the reproducibility of the expert between the two
48 approaches. Significance was tested using a robust test for the equality of variances (Brown and
49 Forsythe test). The confidence interval of the variance ratio was estimated using bootstrap re-sampling
50
51
52
53
54
55
56
57
58
59
60

1
2
3 in 1000 samples. Analysis was performed using Stata version 16 (StataCorp, Texas); a P-value <0.05
4
5 was considered statistically significant.
6
7
8

9 **Results**

10 *Studied population*

11
12 Data from 55 out of the 70 patients recruited in the study were included in the present analysis. The
13
14 baseline demographics of the patients and analysed vessels are shown in Table 1. **Most of the patients**
15
16 **were males, had a family history of coronary artery disease, suffered from hypercholesterolemia and**
17
18 **were in sinus rhythm. The average heart rate was 64±7 (range: 48-78) beats per minute; there was a**
19
20 **balanced representation of the three coronary arteries in the analysis.**
21
22
23
24
25

26 *Conventional versus ED approach*

27
28 The mean length of the analysed segments was 49.96±24.00mm. In the conventional analyses, the first
29
30 frame of the segment of interest coincided in only 6.19% of the cases, while in the ED analyses in all
31
32 cases. The mean distance difference between the location of the first analysed frame in the two
33
34 conventional analyses was 0.19±0.22mm, whereas in the **ED approach** the first frame of the segment of
35
36 interest coincided in all the analyses. The different location of the first frame had an impact on the
37
38 length of the analysed segments; the mean length difference between first and second segmentation in
39
40 the conventional approach was significantly larger than the length difference noted in the **ED approach**
41
42 (Table 2). The ICC was close to 1 in all the volumetric analyses; however, a larger intra-observer
43
44 variability was noted between the estimations of the expert analyst – as indicated by the variance ratio
45
46 – for the normalised lumen and vessel volumes, TAV and the PAV in the conventional than the **ED**
47
48 **approach** (Table 2, Figure 2).
49

50
51 Results were similar for the fixed-length analysis (supplementary file, Table 1, and Figure 3) and when
52
53 the analysis focused on the 10mm most diseased segment. As before, the distance difference between
54
55 the first frame of the most diseased 10mm segment was significantly larger in the conventional than the
56
57 ED analyses (4.96±11.83mm vs 0.65±4.63mm, P<0.001). The different location of the most diseased
58
59 10mm segment in the two conventional analyses resulted in large differences for the estimated lumen
60

1
2
3 and vessel volumes, TAV and PAV (Table 2). Conversely, in the **ED approach**, where the location of
4 the 10mm segment coincided in most of the cases, the intra-observer agreement was high for the
5 measured volumes (Table 2).
6
7
8
9

10 11 **Discussion**

12
13 The present study, for the first time, examined the value of a recently introduced DL methodology that
14 allows retrospective identification of ED frames, for improvement of the reproducibility of IVUS
15 volumetric analysis in native coronary arteries. We demonstrated 1) a high intra-observer agreement
16 for normalised lumen and vessel volumes, as well as the TAV and PAV, that have been extensively
17 used as primary end-points in serial IVUS-based studies assessing the efficacy of novel
18 pharmacotherapies on plaque evolution – in the **ED approach** that is superior to the conventional
19 approach; 2) that these results were consistent when analysis focused on the 10mm most diseased
20 segment which often constitutes a secondary end-point of serial intravascular imaging studies
21 examining the efficacy of emerging therapies in inhibiting plaque evolution, and 3) that the improved
22 reproducibility of the **ED analysis** is due not only to the fact that it overcomes the errors induced by the
23 longitudinal motion of the IVUS catheter and the changes in the lumen dimensions during the cardiac
24 cycle but also to its superior reproducibility in identifying the segment of interest compared to the
25 conventional approach.
26
27
28
29
30
31
32
33
34
35
36
37
38
39

40
41 Cumulative evidence from the early days of IVUS imaging have demonstrated significant changes in
42 the lumen and vessel dimensions during the cardiac cycle. Ge et al. were the first that systematically
43 examined the changes in the left main stem and left anterior descending artery reporting a pulsatile
44 variation in the lumen cross-sectional area of 10% (8). These results were also confirmed by the study
45 of Weismann et al. who included all the three epicardial coronary arteries and reported an average
46 change in lumen, vessel and plaque area of 8.1%, 3.7% and 4.9% respectively (7). These changes were
47 more prominent in disease-free segments and in segments with non-calcified plaques compared to IVUS
48 frames portraying calcific-rich plaques.
49
50
51
52
53
54
55
56

57
58 In addition, studies have shown that there is a longitudinal motion of the IVUS probe with regards to
59 the vessel during the cardiac cycle. Arab Zaden et al. have estimated an average longitudinal motion of
60

1
2
3 the IVUS probe during the cardiac cycle of 1.50 ± 0.80 mm (range 0.5-5.5mm); while Talou et al.
4 confirmed these findings and showed that the longitudinal motion of the IVUS probe varies depending
5 on the studied vessel (6,9).
6
7

8
9 Therefore, it has been speculated that non-gated IVUS analysis, which neglects the cyclic changes in
10 vessel dimensions and the longitudinal motion of the IVUS catheter within the vessel, has a limited
11 reproducibility in assessing PAV (19). However, this hypothesis was not confirmed by the study of
12 Jensen et al. – the only report that compared the reproducibility of IVUS-gated and non-gated
13 segmentation and reported similar intra-observer agreement. A possible explanation of this paradox is
14 the fact that the study was underpowered in detecting statistically significant differences between the
15 two analyses as it included only 19 coronary artery segments (14). In view of these findings, the current
16 recommendation is to analyse IVUS imaging data neglecting the phase of the cardiac cycle at which
17 these images were acquired (15).
18
19

20
21 The present study examined for the first time the value of ED IVUS segmentation, using a newly
22 developed DL methodology for retrospective ED frame detection, in improving the reproducibility of
23 IVUS analysis. We included an appropriately-powered sample size of 97 vessels that were analysed by
24 an expert analyst twice and demonstrated that the ED analysis improves the intra-observer agreement
25 of the expert for the quantification of the normalised lumen, vessel, TAV and PAV. This was attributed
26 to the higher agreement of the ED analyses for the proximal and distal end of the segment of interest
27 that determine its length but also to the longitudinal displacement of the IVUS probe and the cyclic
28 changes in vessel areas during the cardiac cycle as it was demonstrated in the fixed-length analysis. The
29 value of ED approach was more prominent in the quantification of the TAV and PAV in the 10mm
30 most diseased segment, as the conventional approach had a weak reproducibility in identifying its
31 location in the segment of interest.
32
33

34
35 IVUS imaging has been extensively used over the recent years to assess the effect of novel therapies on
36 PAV and provide mechanistic insights about their implications on plaque morphology (1). In these
37 studies, established pharmacotherapies which appeared effective in improving clinical outcomes had a
38 marginal but consistent effect on PAV, resulting in a PAV reduction that ranged from 0.3-1.4% (2,4,20-
39 22). In this setting, IVUS segmentation is essential to be reproducible as the reliability of a change in
40
41
42
43
44
45
46
47
48
49
50
51
52
53
54
55
56
57
58
59
60

1
2
3 PAV will compound error from both measures, impacting on the required sample size. For example,
4 the observed ICC for the PAV of 0.997 for the ED approach and of 0.985 for the conventional approach
5 would reduce to 0.973 and 0.864 for the change in PAV if we assume that the correlation for the PAV
6 between baseline and follow-up IVUS examinations is 0.89 (23,24); this would result in an 11%
7 reduction in the required sample size by using the more reliable measurement (25). Therefore, in order
8 to detect a 1% reduction in the PAV with an 80% power and 5% alpha, we would need to recruit 111
9 patients if the SD is 1.34% for baseline and follow-up measures and the ICC for PAV is 0.985 – as it
10 was reported in our study with the conventional approach – and 100 patients if the ICC for the PAV
11 improves to 0.997 and the SD to 0.59 with the use of an ED approach. Thus, ED analysis should be
12 considered in serial IVUS-based imaging studies as reducing the sample size is anticipated to decrease
13 their cost and expedite patient recruitment.

14
15
16
17
18
19
20
21
22
23
24
25
26
27
28
29
30
31
32
33
34
35
36
37
38
39
40
41
42
43
44
45
46
47
48
49
50
51
52
53
54
55
56
57
58
59
60
The accurate and reproducible quantification of atherosclerotic disease severity using the ED analysis is also likely to enable more accurate estimation of the FFR using IVUS-based computational modelling (26,27). However, this has to be proven in a prospective, appropriately powered clinical study.

Limitations

A major limitation of the present study is the fact we tested the reproducibility of the volumetric analyses in IVUS sequences acquired at one time-point and not in sequential IVUS examinations performed during the index procedure as it has been reported in previous analyses (14,28). It is apparent however that the latter would have been possible only in the context of a prospective, large-scale clinical study with pre-specified imaging end-points. Moreover, we did not test the reproducibility of the two approaches to assess changes in the PAV in patients who had IVUS imaging at baseline and after treatment with medications that inhibit atherosclerotic evolution. In addition, the ED analysis is feasible only for IVUS data acquired by a catheter that is withdrawn at low speed as high-speed IVUS pullbacks would result in acquisition of only a handful of end-diastolic IVUS frames per segment. Furthermore, the study was performed using a high-resolution IVUS system so it is unclear whether the reported results would apply to IVUS data acquired by 20MHz or 40MHz IVUS catheters. Moreover, the DL methodology was developed to detect ED frames in patients in sinus rhythm and was tested in this study in a population that was predominantly in sinus rhythm. Further research is needed to examine its

1
2
3 performance in patients with atrial fibrillation and its value in improving the reproducibility of IVUS
4
5 segmentation in this population.
6
7
8

9 **Conclusions**

10 ED IVUS segmentation enables more reproducible IVUS volumetric analysis allowing accurate
11
12 quantification of the normalised lumen, vessel, TAV and the PAV, compared to the conventional
13
14 approach which is currently used by most core-labs. The superiority of ED analysis should be attributed
15
16 to the higher intra-observer agreement in defining the segment of interest but also to the fact that is not
17
18 susceptible to the longitudinal motion of the IVUS catheter and the cyclic changes in vessel dimensions
19
20 during the cardiac cycle. Therefore, the ED approach should be preferred over the conventional
21
22 approach for the analysis of IVUS data acquired in longitudinal studies assessing the efficacy of focal
23
24 and systemic therapies targeting atherosclerosis.
25
26
27
28
29
30
31
32

33 **Data Availability Statement**

34 Data is readily available upon request
35
36
37
38
39
40
41
42
43
44
45
46
47
48
49
50
51
52
53
54
55
56
57
58
59
60

References

1. Bose D, von Birgelen C, Erbel R. Intravascular ultrasound for the evaluation of therapies targeting coronary atherosclerosis. *J Am Coll Cardiol* 2007;49(9):925-32.
2. Nicholls SJ, Ballantyne CM, Barter PJ, Chapman MJ, Erbel RM, Libby P, Raichlen JS, Uno K, Borgman M, Wolski K and others. Effect of two intensive statin regimens on progression of coronary disease. *N Engl J Med* 2011;365(22):2078-87.
3. Nissen SE, Tuzcu EM, Schoenhagen P, Brown BG, Ganz P, Vogel RA, Crowe T, Howard G, Cooper CJ, Brodie B and others. Effect of intensive compared with moderate lipid-lowering therapy on progression of coronary atherosclerosis: a randomized controlled trial. *JAMA* 2004;291(9):1071-80.
4. Nissen SE, Nicholls SJ, Sipahi I, Libby P, Raichlen JS, Ballantyne CM, Davignon J, Erbel R, Fruchart JC, Tardif JC and others. Effect of very high-intensity statin therapy on regression of coronary atherosclerosis: the ASTEROID trial. *JAMA* 2006;295(13):1556-65.
5. Tardif JC, Gregoire J, L'Allier PL, Ibrahim R, Lesperance J, Heinonen TM, Kouz S, Berry C, Basser R, Lavoie MA and others. Effects of reconstituted high-density lipoprotein infusions on coronary atherosclerosis: a randomized controlled trial. *JAMA* 2007;297(15):1675-82.
6. Arbab-Zadeh A, DeMaria AN, Penny WF, Russo RJ, Kimura BJ, Bhargava V. Axial movement of the intravascular ultrasound probe during the cardiac cycle: implications for three-dimensional reconstruction and measurements of coronary dimensions. *Am Heart J* 1999;138(5 Pt 1):865-72.
7. Weissman NJ, Palacios IF, Weyman AE. Dynamic expansion of the coronary arteries: implications for intravascular ultrasound measurements. *Am Heart J* 1995;130(1):46-51.
8. Ge J, Erbel R, Gerber T, Gorge G, Koch L, Haude M, Meyer J. Intravascular ultrasound imaging of angiographically normal coronary arteries: a prospective study in vivo. *Br Heart J* 1994;71(6):572-8.

- 1
2
3 9. Talou GD, Blanco PJ, Larrabide I, Bezerra CG, Lemos PA, Feijoo RA. Registration Methods
4 for IVUS: Transversal and Longitudinal Transducer Motion Compensation. *IEEE Trans*
5 *Biomed Eng* 2017;64(4):890-903.
6
7
- 8
9 10. von Birgelen C, de Vrey EA, Mintz GS, Nicosia A, Bruining N, Li W, Slager CJ, Roelandt JR,
10 Serruys PW, de Feyter PJ. ECG-gated three-dimensional intravascular ultrasound: feasibility
11 and reproducibility of the automated analysis of coronary lumen and atherosclerotic plaque
12 dimensions in humans. *Circulation* 1997;96(9):2944-52.
13
14
- 15 11. De Winter SA, Hamers R, Degertekin M, Tanabe K, Lemos PA, Serruys PW, Roelandt JR,
16 Bruining N. Retrospective image-based gating of intracoronary ultrasound images for improved
17 quantitative analysis: the intelligate method. *Catheter Cardiovasc Interv* 2004;61(1):84-94.
18
19
- 20 12. Maso Talou GD, Larrabide I, Blanco PJ, Bezerra CG, Lemos PA, Feijoo RA. Improving
21 Cardiac Phase Extraction in IVUS Studies by Integration of Gating Methods. *IEEE Trans*
22 *Biomed Eng* 2015;62(12):2867-77.
23
24
- 25 13. Torbati N, Ayatollahi A, Sadeghipour P. Image-Based Gating of Intravascular Ultrasound
26 Sequences Using the Phase Information of Dual-Tree Complex Wavelet Transform
27 Coefficients. *IEEE Trans Med Imaging* 2019;38(12):2785-2795.
28
29
- 30 14. Jensen LO, Thayssen P. Accuracy of electrocardiographic-gated versus nongated volumetric
31 intravascular ultrasound measurements of coronary arterial narrowing. *Am J Cardiol*
32 2007;99(2):279-83.
33
34
- 35 15. Mintz GS, Garcia-Garcia HM, Nicholls SJ, Weissman NJ, Bruining N, Crowe T, Tardif JC,
36 Serruys PW. Clinical expert consensus document on standards for acquisition, measurement
37 and reporting of intravascular ultrasound regression/progression studies. *EuroIntervention*
38 2011;6(9):1123-30, 9.
39
40
- 41 16. Gerstein HC, Ratner RE, Cannon CP, Serruys PW, Garcia-Garcia HM, van Es GA, Kolatkar
42 NS, Kravitz BG, Miller DM, Huang C and others. Effect of rosiglitazone on progression of
43 coronary atherosclerosis in patients with type 2 diabetes mellitus and coronary artery disease:
44 the assessment on the prevention of progression by rosiglitazone on atherosclerosis in diabetes
45 patients with cardiovascular history trial. *Circulation* 2010;121(10):1176-87.
46
47
48
49
50
51
52
53
54
55
56
57
58
59
60

17. Bajaj R, Huang X, Kilic Y, Jain A, Ramasamy A, Torii R, Moon J, Koh T, Crake T, Parker MK and others. A deep learning methodology for the automated detection of end-diastolic frames in intravascular ultrasound images *Int J Cardiovasc Imaging*. 2021.
18. Ramasamy A, Safi H, Moon JC, Andiapen M, Rathod KS, Maurovich-Horvat P, Bajaj R, Serruys PW, Mathur A, Baumbach A and others. Evaluation of the Efficacy of Computed Tomographic Coronary Angiography in Assessing Coronary Artery Morphology and Physiology: Rationale and Study Design. *Cardiology* 2020;145(5):285-293.
19. De Winter SA, Hamers R, Roelandt JR, Serruys PW, Bruining N. Quantitative gated intravascular ultrasound largely reduces the population size for atherosclerosis progression-regression trials: a computer simulation study. 36th Annual Computers in Cardiology Conference; Park City, UT 2009:829-832.
20. Raber L, Taniwaki M, Zaugg S, Kelbaek H, Roffi M, Holmvang L, Noble S, Pedrazzini G, Moschovitis A, Luscher TF and others. Effect of high-intensity statin therapy on atherosclerosis in non-infarct-related coronary arteries (IBIS-4): a serial intravascular ultrasonography study. *Eur Heart J* 2015;36(8):490-500.
21. Tsujita K, Sugiyama S, Sumida H, Shimomura H, Yamashita T, Yamanaga K, Komura N, Sakamoto K, Oka H, Nakao K and others. Impact of Dual Lipid-Lowering Strategy With Ezetimibe and Atorvastatin on Coronary Plaque Regression in Patients With Percutaneous Coronary Intervention: The Multicenter Randomized Controlled PRECISE-IVUS Trial. *J Am Coll Cardiol* 2015;66(5):495-507.
22. Nicholls SJ, Puri R, Anderson T, Ballantyne CM, Cho L, Kastelein JJ, Koenig W, Somaratne R, Kassahun H, Yang J and others. Effect of Evolocumab on Progression of Coronary Disease in Statin-Treated Patients: The GLAGOV Randomized Clinical Trial. *JAMA* 2016;316(22):2373-2384.
23. Nissen SE, Tuzcu EM, Libby P, Thompson PD, Ghali M, Garza D, Berman L, Shi H, Buebendorf E, Topol EJ and others. Effect of antihypertensive agents on cardiovascular events in patients with coronary disease and normal blood pressure: the CAMELOT study: a randomized controlled trial. *JAMA* 2004;292(18):2217-25.

- 1
2
3 24. May K, Hittner JB. On the relation between power and reliability of difference scores. *Percept*
4 *Mot Skills* 2003;97(3 Pt 1):905-8.
5
6
7 25. Perkins DO, Wyatt RJ, Bartko JJ. Penny-wise and pound-foolish: the impact of measurement
8 error on sample size requirements in clinical trials. *Biol Psychiatry* 2000;47(8):762-6.
9
10
11 26. Yu W, Tanigaki T, Ding D, Wu P, Du H, Ling L, Huang B, Li G, Yang W, Zhang S and others.
12 Accuracy of Intravascular Ultrasound-Based Fractional Flow Reserve in Identifying
13 Hemodynamic Significance of Coronary Stenosis. *Circ Cardiovasc Interv* 2021;14(2):e009840.
14
15
16
17 27. Sakurai S, Takashima H, Waseda K, Gosho M, Kurita A, Ando H, Maeda K, Suzuki A,
18 Fujimoto M, Amano T. Influence of plaque characteristics on fractional flow reserve for
19 coronary lesions with intermediate to obstructive stenosis: insights from integrated-backscatter
20 intravascular ultrasound analysis. *Int J Cardiovasc Imaging* 2015;31(7):1295-301.
21
22
23
24
25
26 28. Rodriguez-Granillo GA, Vaina S, Garcia-Garcia HM, Valgimigli M, Duckers E, van Geuns RJ,
27 Regar E, van der Giessen WJ, Bressers M, Goedhart D and others. Reproducibility of
28 intravascular ultrasound radiofrequency data analysis: implications for the design of
29 longitudinal studies. *Int J Cardiovasc Imaging* 2006;22(5):621-31.
30
31
32
33
34
35
36
37
38
39
40
41
42
43
44
45
46
47
48
49
50
51
52
53
54
55
56
57
58
59
60

Figure legends

Figure 1. A case example showing the segment of interest defined by the conventional and the ED approach. In the ED approach, the proximal and distal end of the segment of interest coincide; conversely, in the conventional approach there was 3 frame difference between the estimations of the expert analyst for the location of the distal end of the segment of interest.

Figure 2. Bland-Altman plots of the % differences of the estimations of the expert analyst for the normalised lumen, vessel, TAV and the PAV in the conventional analysis (A, B, C and D respectively) and ED analysis (E, F, G and H respectively).

Supplementary Figure 1. Methodology applied to identify the 10 sub-segments that will be used to define the distal end of the segment of interest in the second fixed-length analysis using the conventional approach. After the detection of the most distal ED frame – i.e., the frame at the peak of the QRS complex – of the segment of interest using the DL methodology, then the cardiac cycle was split to 10 sub-segments; 5 sub-segments were defined distally and 4 proximally to the ED frame. One of these frames will be considered as the distal end of the segment of interest in the second fixed-length analysis using the conventional approach.

Supplementary Figure 2. Segment of interest defined by the ED and the conventional approach in the fixed-length analysis. The distal end of the segment of interest was similar in the two ED analyses and the 1st conventional analysis. In the 2nd conventional analysis, the distal end of the segment of interest was located 3 frames more proximally – corresponding to the first sub-segment of the period between two end-diastolic frames.

Supplementary Figure 3. Bland-Altman plots of the % differences of the estimations of the expert analyst for the normalised lumen, vessel, TAV and the PAV in the fixed-length analyses for the conventional (A, B, C and D respectively) and the ED approaches (E, F, G and H respectively).

Supplement

End-diastolic segmentation of intravascular ultrasound images enables more reproducible volumetric analysis of atheroma burden

Materials and Methods

DL methodology for ED frame detection

The developed DL methodology for retrospective ED frame detection was trained in NIRS-IVUS imaging data that were co-registered with the concurrent electrocardiographic (ECG)-signal and were acquired from 20 coronary artery segments. The ECG estimations for the ED were used as the reference standard.

The methodology is based on a network model with a bidirectional gated-recurrent-unit (Bi-GRU) structure. The model analyses the whole IVUS sequences to determine patterns of changes in pixel intensity in corresponding pixels between consecutive frames to identify the frame corresponding to ED.

First, the IVUS sequence is pre-processed by a median filter to reduce noise and then the absolute pixel-intensity difference between corresponding pixels in consecutive IVUS frames is calculated and added for each frame across the entire pullback; these data which represents the relative motion of the vessel in relation to the IVUS probe are smoothed by a Hanning smoothing algorithm. The processed values are analyzed by the DL model. A 64-frame segment window is generated that is scanned by a Bi-GRU model which analyses patterns of the changes in pixel intensity to identify the ED frame. This window advances frame by frame sequentially until the entire IVUS pullback is analyzed. For each segment window, the probability that the 32nd frame is the ED frame is calculated; the frames with the highest probability amongst neighboring frames are selected and constitute the network output.

Testing of the DL in the same dataset using the leave-one-out approach demonstrated that the proposed method had an excellent accuracy of 80.4% in correctly detecting the ED frame (1).

Intra- and inter-observer variability of the expert analyst

The intra- and inter-observer variability of the expert analyst for the lumen and EEM borders was examined in 2,437 ED frames obtained from 20 vessels. The analyst detected these borders twice within a 2-month interval and the area estimations between the two analyses were compared. The same dataset was segmented by another expert, and his estimations were compared with the estimations of the first analyst to report the inter-observer variability.

An excellent agreement between expert analyst estimations was found for the lumen and EEM areas (mean difference: $0.07 \pm 0.47 \text{mm}^2$ and $0.09 \pm 0.46 \text{mm}^2$ respectively). The inter-observer agreement of the two experts was also high with the mean difference between observers' estimations being $0.07 \pm 0.65 \text{mm}^2$ for the lumen and $0.10 \pm 0.53 \text{mm}^2$ for the EEM areas.

Fixed-length analysis using the conventional and the ED approach

To estimate the effect of the longitudinal motion of the catheter within the vessel and of the changes in lumen dimensions on volume measurements two analyses were performed.

In the first, the expert analyst identified the ED frame that corresponded to the distal end of the segment of interest and then analysis was performed at 1mm intervals till its proximal end that corresponded to the frame portraying the most distal part of the most proximal side-branch.

The second analysis started from a phase of the cardiac cycle that was not necessarily the ED phase. More specifically, the distal end of the segment of interest in this analysis was estimated using the following approach: the heart rate in each pullback was used to identify the frame interval between two ED frames and this was split in 10 sub-segments. For example, if the heart rate of a patient was 60 beats per minute and the catheter acquired 30 fps then the frame interval between two ED frames is 30 frames and each one of the 10 sub-segments has 3 frames.

Then, 5 sub-segments were defined distally and 4 proximally to the ED frame that corresponded to the distal end of the segment of interest in the first analysis so as the beginning of the second analysis to be close to the first. The frames at the end of the above 10 sub-segments (5 before the ED frame, 1 at ED and 4 proximally to the ED) portrayed the vessel at 10 different phases of the cardiac cycle (Supplementary Figure 1).

1
2
3 In order to have an equal representation of these 10 phases in the second analysis, we implemented the
4 following process: for the first vessel the distal end of the second analysis corresponded to the frame at
5 the end of the 5th sub-segment located distally to the most distal ED frame of the first analysis, for the
6
7 the end of the 5th sub-segment located distally to the most distal ED frame of the first analysis, for the
8
9 second vessel the distal end of the second analysis corresponded to the frame at the end of the 4th sub-
10 segment, for the 3rd vessel to the 3rd sub-segment and so on till the 10th vessel for which the distal end
11 of the analysis corresponded to the frame at the end of the 4th sub-segment located proximally to the
12 distal ED frame of the first analysis. This process was repeated sequentially for all the studied vessels.
13
14 The proximal end of the segment of interest in the second analysis was estimated in such a way so as its
15 length to be equal to the length of this segment in the first analysis (Supplementary Figure 2).
16
17 The reproducibility of the above-mentioned fixed-length conventional analysis was compared with the
18 reproducibility of a fixed-length ED analysis. For this purpose, the expert analyst performed twice the
19 segmentation of the ED frames, identified by the developed DL approach, that were included in the
20 segment of interest which was assumed to have a fixed length.
21
22
23
24
25
26
27
28
29
30
31
32
33

34 **Results**

35 *Fixed-length analysis with the conventional and the ED approach*

36
37 Supplementary Table 1 shows the results of the fixed-length analyses for the conventional and the ED
38 approaches. A high ICC was noted for all the measurements in both approaches. However, the mean±SD
39 of the differences between the two analyses were smaller in the ED approach for all the studied metrics,
40 while the variance ratio indicated that this methodology enables more reproducible volumetric analysis
41 than the conventional approach (Supplementary Figure 3).
42
43
44
45
46
47
48
49
50
51
52
53
54
55
56
57
58
59
60

References

1. Bajaj R, Huang X, Kilic Y, Jain A, Ramasamy A, Torii R, Moon J, Koh T, Crake T, Parker MK and others. A deep learning methodology for the automated detection of end-diastolic frames in intravascular ultrasound images Int J Cardiovasc Imaging. 2021

For Review Only